THE UNIVERSITY OF ALBERTA

PUMPING MECHANISMS IN A HYDROGEN INFRARED LASER

by

AMIN NURDIN DHARAMSI

A THESIS

SUBMITTED TO THE FACULTY OF GRADUATE STUDIES AND RESEARCH

IN PARTIAL FULFILMENT OF THE REQUIREMENTS FOR THE DEGREE

OF MASTER OF SCIENCE

DEPARTMENT OF ELECTRICAL ENGINEERING

EDMONTON, ALBERTA

FALL, 1977

ABSTRACT

Infrared vibrational-rotational transitions in a homonuclear diatomic molecule, can only occur at high pressures and/or in the presence of an external electric field.

Experimental attempts at making a high pressure H_2 laser by using intense β particle radioactive isotopes as a source of preionizing electrons are described.

Resonant Electron-to-Vibrational transfer is also discussed as a possibility for creating a population inversion in H_2. An experiment designed to achieve E-V transfer, from metastable NO_2 electronic states to H_2 vibrations, is described. Experimental values of the self quenching cross-section together with a value for quenching of NO_2^* by H_2 are presented.

Finally, non-resonant Electronic-to-Vibrational energy transfer is discussed. It is shown that resonance is not an important criterion for efficient E-V transfer. The percentage of vibrational energy produced in the quenching of Na^* by H_2 is calculated, and compared with experimental values available. Non-resonant E-V transfer theory is discussed in light of the Born-Oppenheimer Approximation and it is shown how the latter offers a broad basis for selection of suitable pumping atoms or molecules for any potential laser molecule, including H_2.

ACKNOWLEDGEMENTS

The author would like to express his thanks to Dr. J. Tulip who supervised this work.

Assistance of Mr. R. Nieva, especially with the computations involved in this thesis, is greatly appreciated.

Thanks also go to Mrs. B. Gallaiford who typed the manuscript.

TABLE OF CONTENTS

LIST OF TABLES

LIST OF FIGURES

CHAPTER I

INTRODUCTION

High power tunable infra-red lasers would find many uses in research and industry. For example, they would be particularly useful in molecular spectroscopy and biology [1,2], in the field of communications [3] and in isotope enrichment applications [4,8,9].

Output pulses of very short duration (of the order of picoseconds) could be obtained by mode locking such lasers. This follows from the fact that in mode locked operation the output pulse width is inversely proportional to the bandwidth [16], which in a continuously tunable range, could be very large.

Many tunable semiconductor lasers have successfully been put into operation. These presently cover the region of the IR spectrum between about 0.5μm to 50μm [3]. However, the power output levels from such lasers are very low (not exceeding a few dozen watts at the most). This limits their uses considerably [1].

On the other hand, high output power IR gas lasers have been built in recent years. Output powers of up to a few Kilowatts continuous and a few Megawatts pulsed are relatively common from the CO_2 laser. This makes tunable IR gas lasers a particularly attractive proposition.

Basov *et al* [1,5] have pointed out the possibility of making tunable CO and H_2 lasers by utilising pressure broadening of the spectral lines so that adjacent lines overlap, producing a continuous amplification band.

Continuously tunable high pressure CO_2 lasers have been reported by T.Y. Chang and O.R. Wood [10], by A.J. Alcock *et al* [11] and by N.G. Basov *et al* [12]. Chang and Wood used the 4.2μm radiation from a

Hydrogen Bromide pulsed laser to optically pumped pure CO_2 at 33 Atmospheres. Alcock *et al* used UV photopreionization to obtain continuous tuning over a range of about $20cm^{-1}$ at 15 Atmospheres. Basov *et al* obtained operation around 50 Atmospheres by using the e-beam technique resulting in a tunable range of about $100cm^{-1}$.

For a CO laser a pressure of between 10 to 15 Atmospheres would be high enough to produce a continuous band [1].

It is shown below that a pressure of about 40 Atmospheres would suffice for the H_2 laser. A tunable H_2 laser has not been reported yet.

A Hydrogen laser operating on vibrational rotational transitions would emit radiation in the near IR (at around 2μm) [18].

(Bazhulin *et al* [6] have achieved lasing action in H_2 and D_2 around the 1μm region. Population inversion between the vibrational rotational levels of the first two excited *electronic* states was obtained by making use of the Franck-Condon Principle and the fact that the minima of these two states occur at different internuclear separations. The method of excitation was by an electric discharge at 35KV and 20Hz at relatively low pressures [7]).

Some IR lasers together with their output wavelengths are listed in Appendix I.

IR H_2 laser transitions between vibrational-rotational levels would not occur under ordinary circumstances because, being a homonuclear diatomic molecule, H_2 does not have a permanent dipole moment, and the dipole transition probability is zero, such transitions being "forbidden" [13]. An electric dipole moment could, however, be induced in the molecule by an external electric field (d.c. or a.c.) [5] or by intermolecular collisions [14] giving a nonzero, although small, probability for such transitions. Basov *et al* [5] have suggested that the strong electric

field of CO_2 laser radiation combined with the isotope effect in the unsymmetrical HD molecule (which has a dipole moment in the non zero vibrational quantum states [13]) could be used to make a high pressure Hydrogen laser. Christensen and Greenfield [14] have analysed a hypothetical H_2 laser that utilises both the collision induced dipole (cid) and the electric field induced dipole (efi) effects.

1.1 Scope of this Work

A condition for continuous tunability in a gas laser is derived below. It is shown that a Hydrogen laser operating at a pressure around 40 Atmospheres would be continuously tunable.

Chapter II deals with experimental attempts at obtaining a high pressure discharge in Hydrogen and other gases by using an intense radioactive β particle emitter for preionization.

Chapter III describes an experiment designed to optically pump the Hydrogen molecule by resonant E-V transfer from NO_2 excited metastable states. Experimental cross-section values for the quenching of these NO_2 states by collision with other NO_2 molecules and with H_2 molecules are presented.

The general theory of E-V transfer is described and applied to some systems containing Hydrogen molecules in Chapter IV. The results obtained in Chapter III are discussed in light of this theory and it is shown that resonance between electronic and vibrational levels is not as important a condition for efficient E-V transfer as is generally thought. Cross-sections for the E-V transfer process are calculated for a few systems. These calculations are used as a basis for suggesting some atoms that

could transfer electronic energy to Hydrogen vibrational levels.

Finally a summary is presented in Chapter V together with some suggestions on how the present work might be extended.

1.2 Condition for Continuous Tunability

When a radiating atom or molecule suffers a collision with another particle, the perturbation causes an interruption in the emitted "wave train". A Fourier transform of this train reveals additional frequencies that would not be present if no collision had occurred [17]. The emitted line is therefore ("collision" or "pressure") broadened. If the consequent increase in line widths is large enough, adjacent lines overlap and the emitted spectrum would then become a continuous band.

It can be shown that the profile of a pressure broadened line is Lorentzian [17] and is given by

$$g(\nu) \simeq c \frac{1}{(\Delta\nu)^2 + (\frac{1}{2\pi T_o})^2} \qquad (1.1)$$

where

c is a constant incorporating the oscillator strength of the particular transition under consideration,

ν is the frequency,

ν_o is the centre frequency of the profile,

T_o is the mean free (or "flight") time between collisions

and

$\Delta\nu = \nu - \nu_o$

($g(\nu)$ is symmetrical about and has a maximum at ν_o).

From (1.1) it follows that the half intensity linewidth $\Delta\nu_{hw}$, is given by

$$\Delta\nu_{hw} = \frac{1}{2\pi T_o} \qquad (1.2)$$

Also, from the definition of T_o, it follows that the average number of collisions per unit time, denoted by S, is given by

$$S = \frac{1}{T_o} \tag{1.3}$$

If the cross-section for broadening collisions is σ_b, v the mean relative speed of the particles and N their concentration, then

$$S = \frac{1}{T_o} = \sigma_b \; v \; N \tag{1.4}$$

From (1.2) and (1.4), it is seen that the half line width is proportional to the gas pressure at a given temperature (This assumes that σ_b is not a strong function of pressure). Further, in a gaseous mixture the half width of a line is equal to the sum of half widths due to each component of the mixture, considered separately.

Equations (1.2), (1.3) and (1.4) can be combined with the ideal gas relation [19]:

$$P = NKT \tag{1.5}$$

to give

$$\frac{\Delta\nu_{hw}}{P} = \frac{1}{2\pi} \; \sigma_b \; v \; \frac{1}{KT} \tag{1.6}$$

For a given temperature, this ratio is approximately constant in a given pressure range, if σ_b is regarded as the mean collision cross-section in this range.

For a gas like CO the constant ratio in (1.6) is of the order of 10^7 Hz/torr [1].

Now v is inversely proportional to the square root of the mass of the colliding molecules; this follows from the kinetic theory of gases [17]:

$$v = \left(\frac{8KT}{\pi M_o} \right)^{1/2} \tag{1.7}$$

We deduce, therefore that for H_2 the broadening per unit frequency, $(\Delta\nu_{hw}/P)$, would be approximately $10^7 \left(\frac{M_{CO}}{M_{H_2}}\right)^{1/2}$ where M_{CO} and M_{H_2} are the molecular weights of CO and H_2 respectively. This yields

$$\frac{\Delta\nu_{hw}}{P} \simeq 3.7 \times 10^7 \text{Hz/torr} \tag{1.8}$$

for H_2.

We will use equation (1.8) to estimate the pressure at which continuous tunability may be achieved in a Hydrogen laser. It is first shown below that to achieve overlap between the adjacent vibrational-rotational bands, it is only necessary to broaden the lines by an amount approximately equal to the rotational constant, B, of the molecule.

A diatomic may be regarded as an anharmonic oscillator, the anharmonicity being due to the deviation of the potential curve of the molecule from the simple harmonic potential. This results in an uneven spacing of the vibrational levels, the higher ones being closer together than the lower ones [20]. In the Morse-Oscillator model (where the potential curve under the influence of which the diatomic is vibrating is assumed to be the Morse potential) the magnitude of this anharmonicity ΔE, is given by [1]

$$\Delta E = \left(\frac{h\omega_{1,0}}{2D} \right)^2 \qquad (1.9)$$

where

$\omega_{1,0}$ is the (radian)frequency of the 1→0 transition,

D is the dissociation energy of the molecule.

The lines due to adjacent vibrational transitions do not, ordinarily, coincide because of this anharmonic defect. The separation (in frequency) $\Delta\nu$, between them is given by

$$\Delta\nu = \frac{\Delta E}{h}$$

If each line in this vibrational spectrum were broadened by this amount, the adjacent vibrational levels would overlap. The anharmonic defect is of such a magnitude that it would be necessary to have pressures of the order of hundreds of atmospheres for the desired overlap to occur.

Fortunately however, since each vibrational level has a rotational fine structure, in practice it is not necessary (for the case of H_2 and CO at least) to broaden the lines by ΔE.

Because of the statistical profile of the kinetic energy distribution amongst the molecules of a gas, it turns out that each vibrational level is accompanied by a spectrum of rotational levels excited in the frequency interval $\Delta\Omega \simeq \frac{KT}{h}$ [1] i.e. in the energy interval $\Delta E_R \simeq KT$. At 300°K, this works out to be about 3×10^{-2} ev. If $\Delta E_R \gtrsim \Delta E$ then we may expect overlap between adjacent vibrational levels even if each rotational line was broadened enough to overlap only the next rotational line in the same vibrational level [1]. For H_2 and CO, the value for the anharmonic

defects are found from (1.9), to be about 5×10^{-2} ev and 2×10^{-3} ev. (The values for $\omega_{1,0}$ and D being obtained from Herzberg [18]).

The value for the anharmonic defect in Hydrogen (5×10^{-2} ev) is of the same order of magnitude as the value for spread in excited rotational energy levels (3×10^{-2} ev) (see also Appendix II). The value for the defect in CO (2×10^{-3} ev) is less than ΔE_R (3×10^{-2} ev). Hence, for both these molecules it is only necessary to broaden each line by a value approximately equal to B, the rotational constant, (this being, approximately, the separation between rotational lines).

The values of B for H_2 and CO are 3.6×10^{-3} ev and 2.4×10^{-4} ev corresponding to the frequency spreads of 10^{12} Hz and 10^{11} Hz respectively.

Finally, using the values 4×10^7 Hz/torr (from 1.8) and 10^7 Hz/torr (from Basov *et al* [1]) for these two molecules we find that pressures of about 40 Atmospheres and 13 Atmospheres, respectively would suffice to produce continuous vibrational rotational spectra in these two molecules.

1.3 Condition for Population Inversion

Homonuclear diatomics like H_2 have long vibrational-translational relaxation times because dipole transitions are "forbidden". Rotational-translational relaxation times are, at 300°K and up to several atmospheres, many orders of magnitude smaller. Hence, when considering the interaction of these three types of energies (translational, vibrational and rotational) it might be assumed that the (translational) temperature of the gas, T, is equal to the rotational temperature T_r (as defined below). [T may be defined in the kinetic theory of gases by equation (1.7) above] [5].

The number of molecules in the rotational level J, in the lowest vibrational state is given by [18]

$$N(J) = \frac{NhcB}{KT_r} (2J + 1) \exp\{- \frac{BJ(J + 1)}{KT_r}\} \qquad (1.10)$$

where

N is the total number of molecules, c the velocity of light and the other terms have been defined before.

This Boltzman distribution defines the rotational temperature, T_r. Further it is generally a good approximation to equate T_r with T [5].

The vibrational temperature, T_v is defined as follows [5]:

$$\frac{N_2}{N_1} = \exp(- \Delta E_v / KT_v) \qquad (1.11)$$

where

N_2 and N_1 are the concentration of molecules in the first vibrationally excited and the vibrational ground states respectively,

ΔE_v is the energy separation between these two levels.

Now, vibrational-rotational transitions in molecules which have had a dipole moment induced by either the efi or cid effects must satisfy the following selection rules: [14]

$$\Delta V = 0, \pm 1 \qquad (1.12)$$

$$\Delta J = 0, \pm 2 \qquad (1.13)$$

where

V and J are the vibrational and rotational quantum numbers, respectively. (The Raman transitions follow the same selection rules).

Consider such a transition between two levels J_2 and J_1 such that

$$J_1 = J_2 + 2 \tag{1.14}$$

Then from (1.10)

$$\frac{N(J_2)}{N(J_1)} = \frac{N_2}{N_1} \cdot \frac{(2J_2+1)}{(2J_1+1)} \exp\left[\frac{-B}{KT_r}\{J_2(J_2+1) - J_1(J_1+1)\}\right]$$

$$= \frac{N_2}{N_1} \cdot \frac{(2J_2+1)}{(2J_1+1)} \exp\left[- \frac{\Delta E_r}{KT_r}\right]$$

where

ΔE_r is the energy difference between the two rotational levels. (We have assumed that the rotational constant B for both the vibrational states is the same). Substituting for $\frac{N_2}{N_1}$ from (1.11) gives

$$\frac{N(J_2)}{N(J_1)} = \exp\left(- \frac{\Delta E_v}{KT_v} \right) \exp \frac{1}{K} \left[- \frac{\Delta E_v}{T_v} - \frac{\Delta E_r}{T_r} \right] \tag{1.15}$$

or

$$\frac{N(J_2)}{N(J_1)} = \exp\left\{ - \frac{\Delta E_v}{KT_v} + \frac{B}{KT_R} (4J_2+6)\right\} \tag{1.16}$$

where we have used (1.14) and the approximation $\frac{(2J_2+1)}{(2J_1+1)} \simeq 1$ which holds for the higher rotational levels. From (1.15) and (1.16) we can write the condition for population inversion $[N(J_2) > N(J_1)]$ in the following equivalent forms [5, 14]:

$$T_v \geq T \frac{\Delta E_v}{B(4J_2+6)} \tag{1.17}$$

or

$$\frac{T_v}{T} \geq \frac{\Delta E_v}{\Delta E_r} \tag{1.18}$$

where the approximation $T_r \simeq T$ has been used.

Equation (1.18) implies that no Q branch ($\Delta J = 0$) transitions could occur because for such transitions $\Delta E_r = 0$.

However, if in the transition process translational energy plays a part, as is the case for cid transitions, then equation (1.18) is modified as follows [14]

$$\frac{T_v}{T} \geq \frac{\Delta E_v}{(\Delta E_r + \Delta E_t)} \tag{1.19}$$

where ΔE_t is that change in translational energy that accompanies the particular vibrational rotational transition under consideration.

This means that a population inversion may exist even when $\Delta E_r = 0$. Further, this inversion could be significant at a low temperature, T. This "translational partial inversion" allows Q branch transitions [14].

It should be pointed out that conditions (1.18) and (1.19) have been derived assuming that the vibrational levels are populated according to the Boltzman distribution (1.11) This is true if the molecules are considered as harmonic oscillators. In that case,Landau and Teller have shown that vibrational relaxation of the molecules may be described by one overall relaxation rate [46]. Hence, although the relaxation times of different vibrational levels of the harmonic oscillator are different, they fit together in such a way that one overall rate relaxation time could be defined for all the transitions.

Treanor *et al* [64] have shown that if anharmonic effects are considered, the distributions could show substantial departure from the Boltzman scheme. Under these conditions, the Landau-Teller model is not quite accurate.

Fortunately, it turns out that the anharmonic effect is advantageous to the process of establishing a population inversion especially in the important case of low translational temperature, since then the populations of the lower vibrational states can be considerably smaller than those predicted by the Landau-Teller model [64].

CHAPTER II

ELECTRIC DISCHARGE EXPERIMENTS

Pumping a laser gas by creating a discharge has been demonstrated to be an efficient technique. High powered efficient CO_2 lasers have been successfully put into operation by this means. Seguin and Tulip [21] obtained increased discharge stability and large discharge energies by incorporating U-V spark radiation for initiating and sustaining the discharge. This method was later used by Alcock *et al* to obtain lasing action at pressures up to 15 Atmospheres in CO_2 [11]. Tulip, Seguin and Faszer [22] used the technique to obtain a high repetition rate (up to 4000 pulses per second) TEA laser.

An extensive quantitative investigation of the radiation from a spark gap and its effect on the CO_2 laser mix was carried out by Seguin, Tulip and McKen [23]. It was found,for example, that the absorption length of the U-V radiation at 200 torr (in a 1:1:1 and a 1:1:3 ratio with tripropylamine additive) was about 5 cm. With some other additives it could be as long as 35 cm.

If the preionization technique is to work at high pressures (at several tens of Atmospheres) then it would be necessary to use much harder radiation to obtain the required longer propagation lengths. It can be shown for example, that soft x-rays in the region between 0.5Å and 1.5Å would have propagation lengths between about 30 cm to about 2 cm at 50 Atmospheres in air. Such wavelengths could be obtained from an x-ray tube operating between 20 and 50 KV. (X-rays produced below 70 KV dissipate most of their energy by ionizing the absorbing molecules [24])

Another source of electrons for preionization would be a radioactive β particle emitter like Strontium 90 (Sr^{90}). The daughter product of this isotope, Yttrium 90 (Y^{90}) is also a β particle emitter. The average β particle energy from Strontium 90 is about 0.18 MeV. Such electrons would have an average absorption length of about 2 cm in 50 Atmospheres of air [26]. The β particles from Y^{90} are on the average about four times as energetic as those from Sr^{90} and would therefore have an absorption length of about 8 cm under the same conditions. The absorption lengths in any laser mix would be different from these figures. However, in the absence of specific data for such gases as H_2 and CO_2, the absorption lengths for air, mentioned above, were used as the basis for selecting Sr^{90} for the experiments described below. The other main reason for selecting this particular isotope was that it could be purchased commercially.

2.1 The Experiment

As pointed out previously, a Hydrogen infra-red laser would have to be operated at a pressure high enough for the collision induced dipole moment to be substantial. The pressure chamber (shown below) was designed to withstand pressures up to 50 Atmospheres.

At these high pressures (tens of Atmospheres) a high voltage pulse of small time duration and a strong source of preionization would be necessary. Each of these factors is dealt with below.

2.1.1 Voltage Requirements

The magnitude of the electric field strength required was calculated

using the Raether Breakdown Criterion [28] for Helium and air, data on Hydrogen being insufficient. See Figure 2.1.

The criterion can be written as

$$\alpha d_c \simeq 17 + \ell n d_c \qquad (2.1)$$

where

α is Townsend's first ionization coefficient (in cm^{-1}),

d_c is the (critical) avalanche length (in cm) at which the avalanche space charge field becomes comparable to the externally applied field.

The numerical value given on the right hand side of equation (2.1) varies slightly with different gases [28], but the variation is small enough not to seriously affect the estimated value for the field.

Equation (2.1) was used in conjunction with the Townsend equation

$$\frac{\alpha}{p} = A \exp(-Bp/E) \qquad (2.2)$$

where

p and E are the pressure and field intensity respectively,

A and B are constants depending on the gas and the value of E/p.

The breakdown field intensity for He at 50 Atmospheres, using equations (2.1) and (2.2) is about 120 KV/cm. This figure was used as a rough target for the Marx generator that was made for the experiment (see Appendix 4). The latter was successfully operated to give output voltages higher than 150 KV.

The voltage pulse duration is important in any gas discharge. Rogoff [30] has shown that thermal instabilities develop in a 500 torr Hydrogen discharge in a time interval of about 100 ns leading to arcing. In the experiment an attempt was made to decrease the pulse width as much as possible by reducing the inductance loop areas.

2.1.2 Preionization Requirements

An approximate condition for the minimum preionization density, n_o, required to initiate a glow discharge is that the avalanche head's radial extension, r, be greater or equal to the dimension $(n_o)^{-1/3}$ [31].

$$r = (d_c \bar{\lambda})^{1/2} \tag{2.3}$$

where

d_c is the extent of the avalanche along the field direction at breakdown and $\bar{\lambda}$ is the mean free path of the electrons [32]. Hence the criterion for minimum preionization density is

$$(n_o)^{-1/3} \lesssim (\bar{\lambda}\, d_c)^{1/2} \tag{2.4}$$

Since $\bar{\lambda}$ is inversely proportional to pressure this may be rewritten as

$$(n_o)_P^{-1/3} \lesssim \left(\frac{\bar{\lambda}_A}{P}\, d_c\right)^{1/2} \tag{2.5}$$

where

$\bar{\lambda}_A$ is the mean free path at atmospheric pressure and $(n_o)_P$ the minimum preionization density at P atmospheres. [$\frac{\bar{\lambda}_A}{P}$ has the unit of length since P is a number in (2.5)].

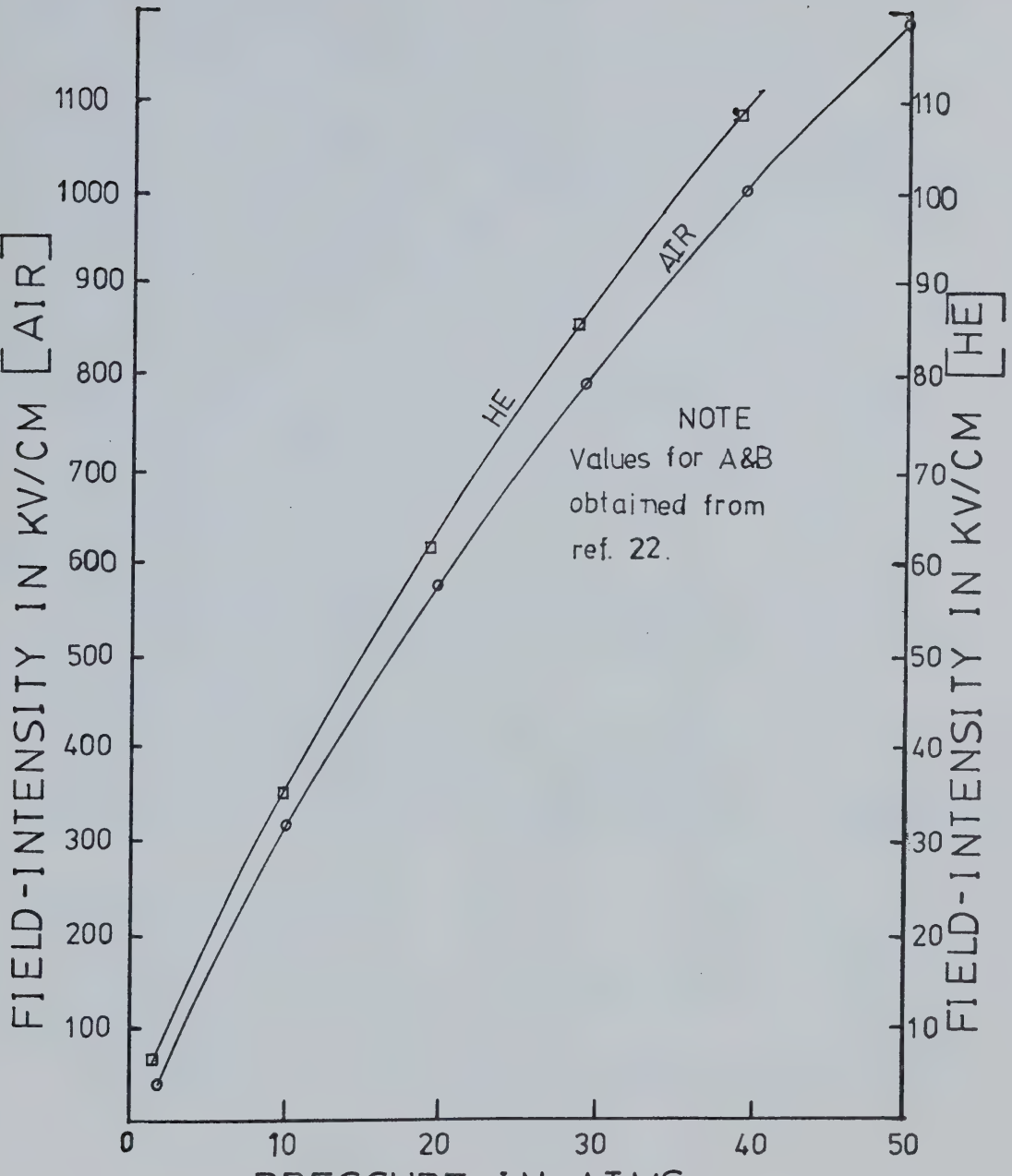

FIG 2·1 COMPUTED BREAKDOWN FIELD STRENGTH VS. PRESSURE

For a CO_2 TEA laser Palmer [31] finds n_o to be about 10^4 cm^{-3}. Hence at 50 Atmospheres $n_o \simeq 4 \times 10^6$ cm^{-3}.

The Sr^{90} sources used each had a dosage of 80 mRad $(sec)^{-1}$. (By definition, 1 Rad is the unit of dose that corresponds to an absorption of 100 ergs in one gram of absorbing medium [33]). Each source irradiated about 50 $(cm)^3$ in the discharge chamber. Using the value of 15.4 ev as the ionization energy of H_2, it follows that the β sources produce electrons at the rates of 10^9 $(cm^{-3})(sec)^{-1}$ and 10^7 $(cm)^{-3}(sec)^{-1}$ in Hydrogen at pressures of 50 Atmospheres and 1 Atmosphere respectively.

These figures ignore secondary ionization processes like emission from the cathode. Losses due to attachment, on the other hand, are not considered either.

The steady state electron concentrations would be close to these numerical values (i.e. 10^9 cm^{-3} and 10^7 cm^{-3}) since the β radiation from the isotopes is continuous.

It is seen therefore that the Sr^{90} source would probably provide enough preionization density for a discharge in Hydrogen at 50 Atmospheres.

2.2 Experimental Procedure

The experimental set up is shown in Figure 2.2 below. The Marx Generator is described in Appendix 4.

The details of the Pressure Chamber are shown below in Figure 2.3.

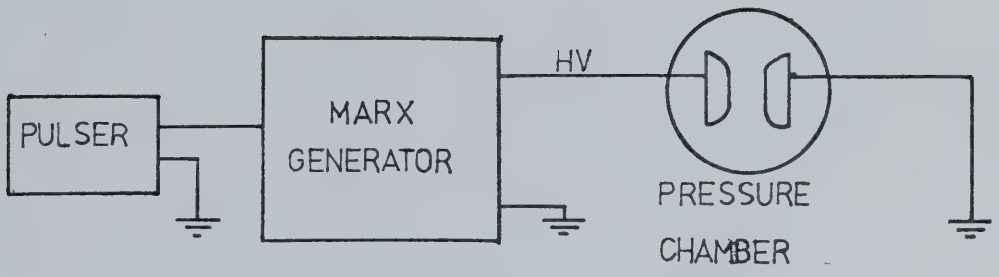

Figure 2.2 A Schematic Diagram of the Apparatus

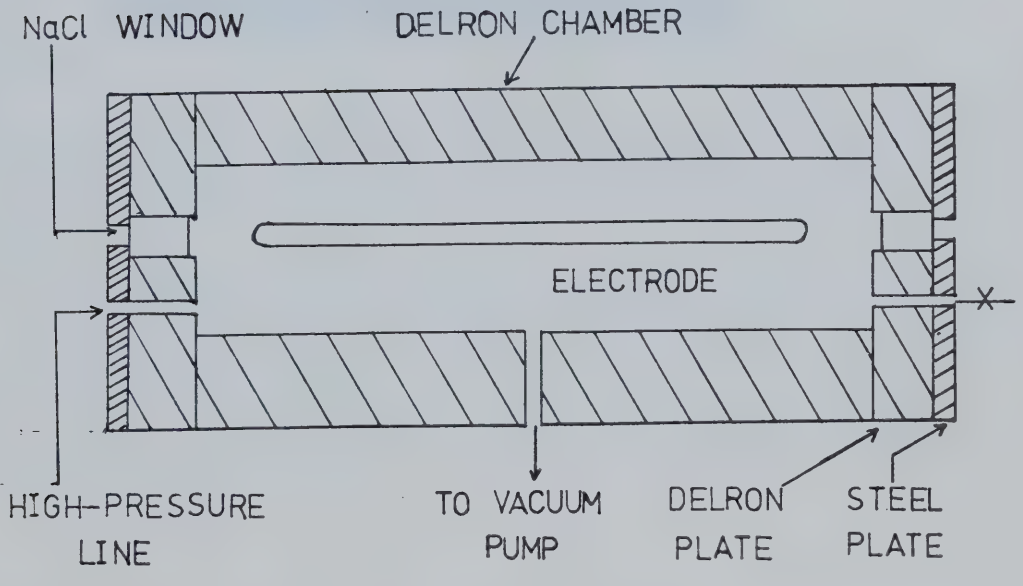

Figure 2.3 Details of the Pressure Chamber

2.3 Results

a) Experiments with Helium:

A glow discharge was obtained in Helium up to pressures of 300 psi gauge (about 22 Atmospheres). The resulting current pulses are shown in Figures 2.4 and 2.5 below.

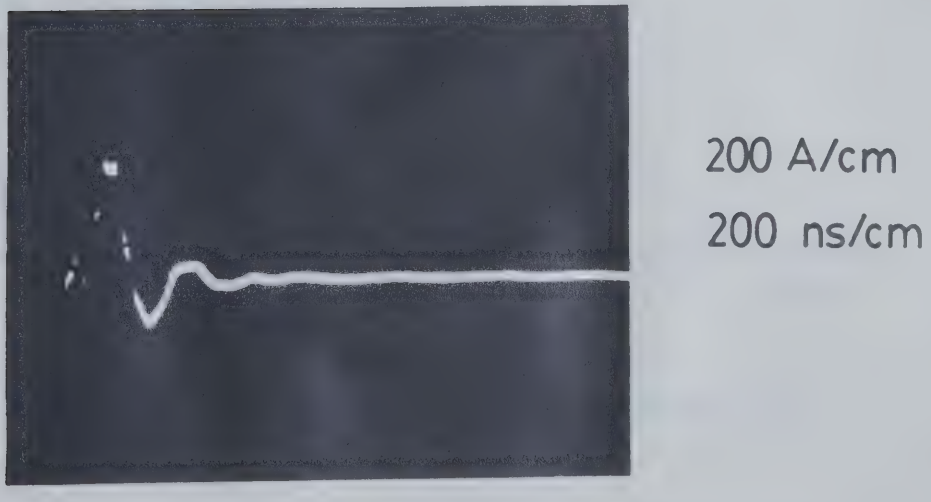

Figure 2.4 Current Pulse Through Helium Discharge at 30 psi Gauge

The discharge deteriorated at pressures of 350 psi and higher.

The electrodes used were Aluminium, Rogowski profiled [27] for 1 cm separation. The discharge seemed, however, to improve when the gap separation was about 2.5 cm.

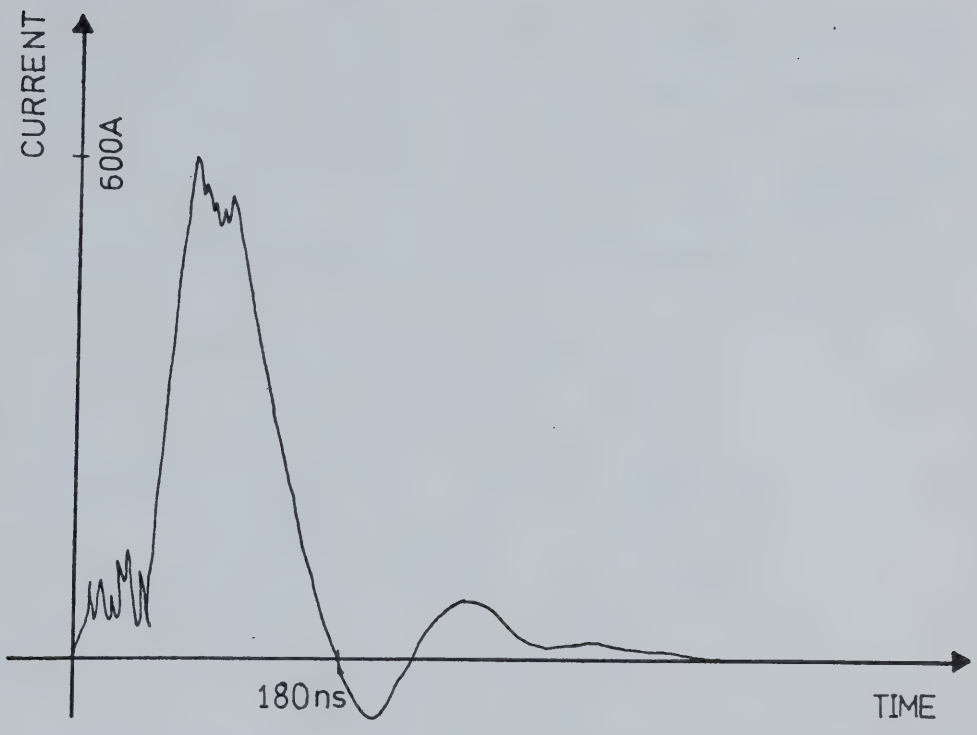

Figure 2.5 Current Pulse Through Helium Discharge at 300 psi Gauge

Bigger electrodes (Aluminium, Rogowski profiled for 2.5 cm - 1 inch - separation) did not improve the discharge by any noticeable amount.

The presence of the Strontium 90 sources did not have much effect either, and the discharge still deteriorated at pressures in excess of 300 psi gauge. Six Strontium sources were used in two different positions as shown below in Figure 2.6.

It was noted that when the interelectrode distance was reduced to below about 1.5 cm arcing occurred.

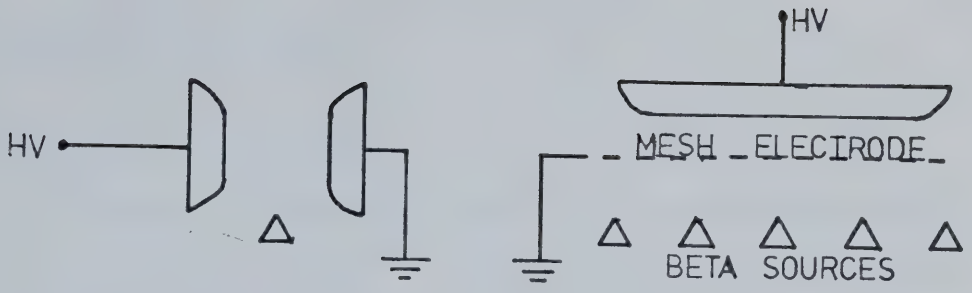

Figure 2.6 Positions of the Strontium 90 Sources

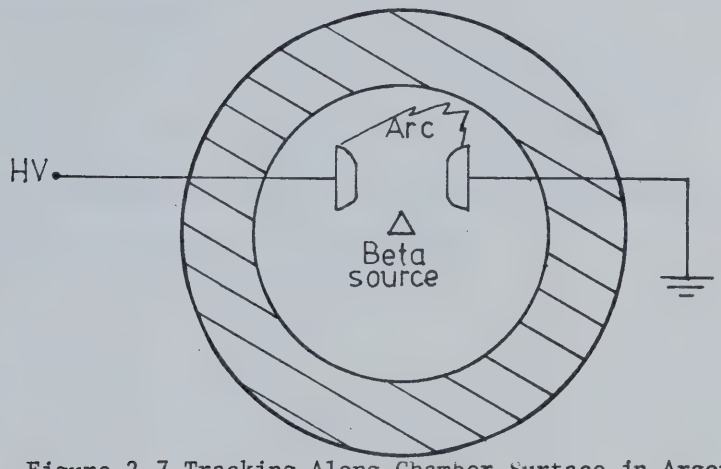

Figure 2.7 Tracking Along Chamber Surface in Argon

b) Experiments with Argon

The above mentioned procedure for Helium was repeated with Argon at pressures between 10 torr to 2 Atmospheres. Arcing was observed every time.

Argon would be very useful in any H_2 laser operating as a cid/efi laser, because of its high polarizability [14].

The arcs, for interelectrode distances larger than 3 cm, (using the electrodes designed for a 2.5 cm gap) occurred on the inside of the chamber surface facing the β sources (See Figure 2.7).

This was probably due to static charge accumulation because of β particle

bombardment of the chamber.

c) Experiments with Hydrogen

The above experiments were repeated with Hydrogen-Helium mixtures. (The minimum partial pressure of Hydrogen experimented with was 5 psi while the maximum partial pressure of Helium used was 50 psi). Arcing occurred every time.

d) Experiments with a Ballast Resistor Electrode

Nineteen 20KΩ (5W) ohmite resistors were employed to make the resistor electrode shown in Figure 2.8.

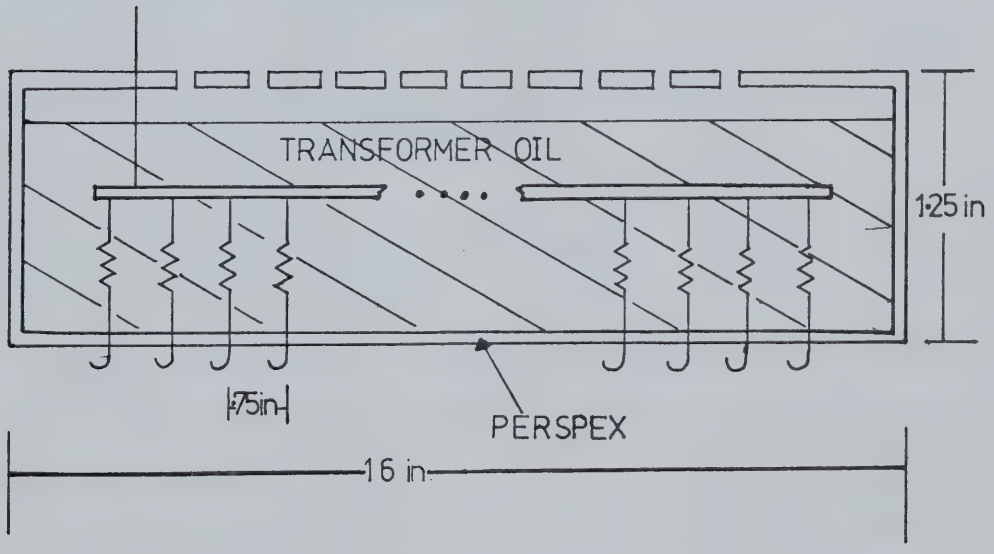

Figure 2.8 Ballast Resistor Electrode

This electrode was used in conjunction with a fine copper wire mesh electrode [shown in Figure 2.6(b) above]. The experiment was repeated with and without the β ray sources. (See Figure 2.9).

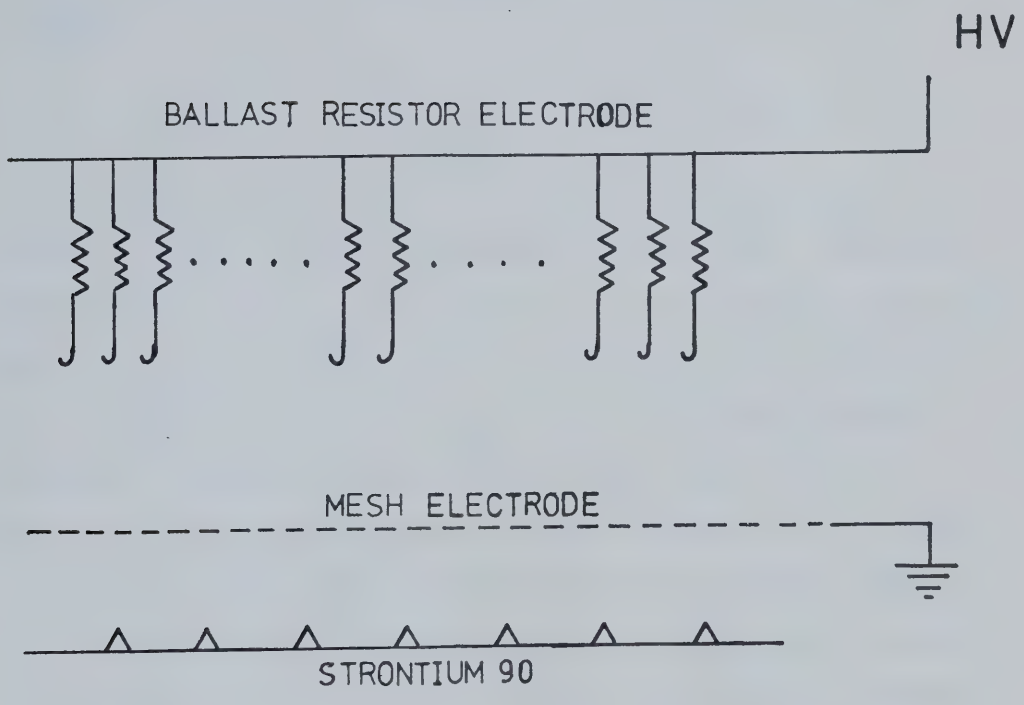

Figure 2.9 Position of Sr^{90} Sources

Without the radioactive sources, it was observed that the presence of even a very small amount of Hydrogen (< 1 psi) in a Helium discharge, resulted in arcing.

The radioactive sources behind the mesh cathode did not improve the discharge in any significant manner.

2.4 Discussion

The experimental breakdown field strength in Helium is in agreement (to within 20%) with the value obtained from Raether's Criterion. Thus, the breakdown field intensity for He at 300 psi from Figure 2.1 is about 75KV/cm, while the experimental value obtained is 60 KV/cm ($\simeq \frac{150KV}{2.5\ cm}$)

Effect of Dissociation on H_2 Discharge:

One reason why it is difficult to obtain a glow discharge in Hydrogen is because it shows dissociative attachment [29]. Attachment leads to a loss of electrons as carriers since the resulting negative ions have a much smaller mobility. It also tends to increase carrier loss due to recombination since the cross-section for the latter process increases. Furthermore, assymetric space charge fields caused by attachment can create instabilities leading to a glow-to-arc transition.

Table 2.1 below, shows the dissociation and ionization energies of a few diatomic molecules including Hydrogen. It is seen that the ratio of dissociation energy to ionization energy is lowest for the Hydrogen molecule (28%). Oxygen is the next lowest with a ratio of 0.41 (41%). In a discharge, therefore, Hydrogen would probably dissociate first before it ionizes. The fact that the Hydrogen atom is very electronegative makes matters worse.

It appears that, although some improvement in the discharge quality might have been obtained if a narrower voltage pulse had been used (instead of the 200 ns pulses obtainable from the Marx), the major difficulty was caused by the effect of dissociative attachment. The strong β particle

Table 2.1 Ionization and Dissociation Energies for Some Diatomics

Molecule	Ionization Energy, I(eV)	Dissociation Energy, D(eV)	$\frac{D}{I}$
O_2	12.5	5.1	0.41
N_2	15.6	9.6	0.61
H_2	15.4	4.36	0.28
CO	14.0	11.1	0.79

sources were not capable of making up for the electron losses due to this phenomenon.

CHAPTER III

EXPERIMENTS ON RESONANT E-V TRANSFER

This Chapter describes experiments designed to pump the vibrational levels of H_2 by resonant transfer from an electronically excited species. NO_2 vapour was excited by radiation from an Argon ion laser. The excited molecule was quenched by H_2 in the experimental chamber. Values for the self quenching cross-section and the quenching cross-section with H_2 are presented.

It is known that NO_2 has metastable electronic states (with lifetimes between 55μs to 70μs) which fluoresce in the red with maximum intensity peaks around 6400Å and 5900Å [34, 35, 36]. These correspond to radiation wavenumbers equal to 15,600 cm^{-1} and 16,950 cm^{-1} respectively. The third and fourth vibrational levels of the ground electronic state of H_2 lie around 14,000 cm^{-1} and 17,000 cm^{-1} [18]. It is seen, therefore, that the fluorescence from NO_2 matches closely with these vibrational levels. The fact that NO_2 is a vapour at low pressures (less than 50 torr) and room temperature and that it absorbs in the visible [37] makes it a suitable material to experiment with.

Dickens, Linnet and Sovers [38] have considered the quenching of an electronically excited atomic species by a diatomic. They considered the case where the total interaction potential curves of the final and initial states are parallel. Although the quenching cross-sections are generally small, a resonance effect is exhibited. Thus the maximum cross-section occurs when the energy defect is zero. Dickens *et al* used a simplified model (taking all the electronic states to be spherically symmetric). Even though the NO_2-H_2 system is more complicated the theoretical

results of Linnet *et al* are of general enough validity [39] to justify experiments of the type described below.

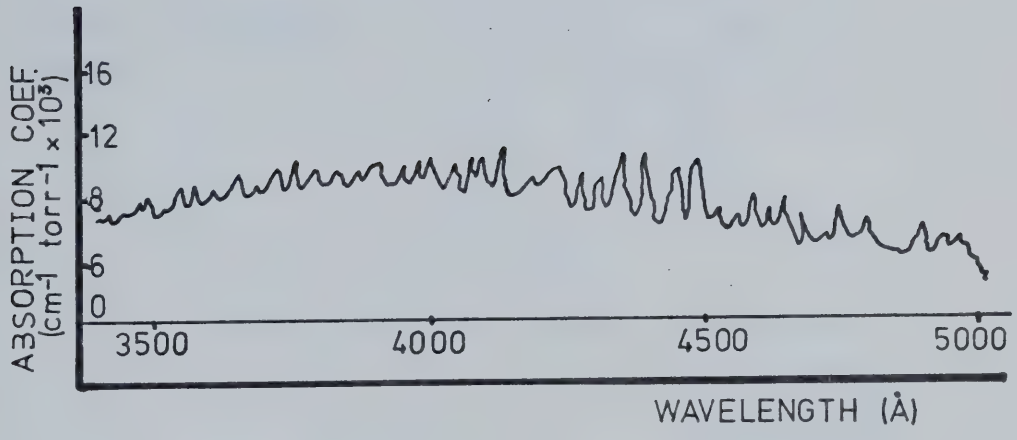

Figure 3.1 Absorption Spectrum of NO_2

3.1 Experimental Investigation of Quenching Cross-Sections

The radiation from the Ar^+ laser consisted of the following six wavelengths: 5145Å, 5017Å 4965Å, 4880Å, 4765Å and 4579Å. Most of the laser power (about 200 mW continuous) was concentrated in the 4880Å and 5145Å lines.

The test chamber was evacuated and then filled with NO_2 at different pressures.

The photomultiplier tube was used in conjunction with a 6180Å (red) filter to cut off any scattered light from the laser. This ensured that

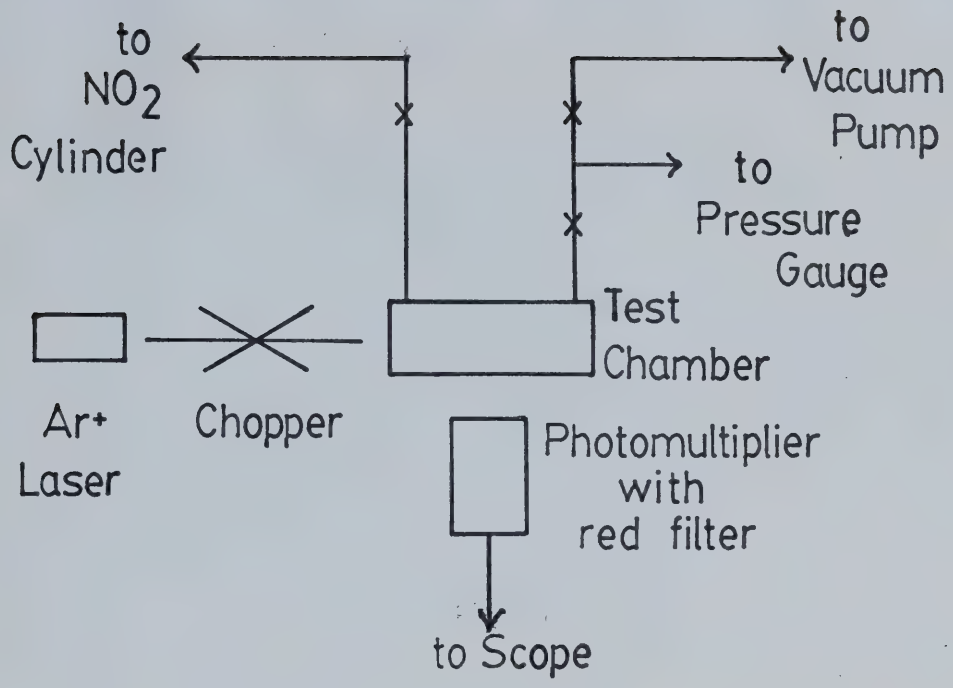

Figure 3.2 Schematic Diagram of the Apparatus

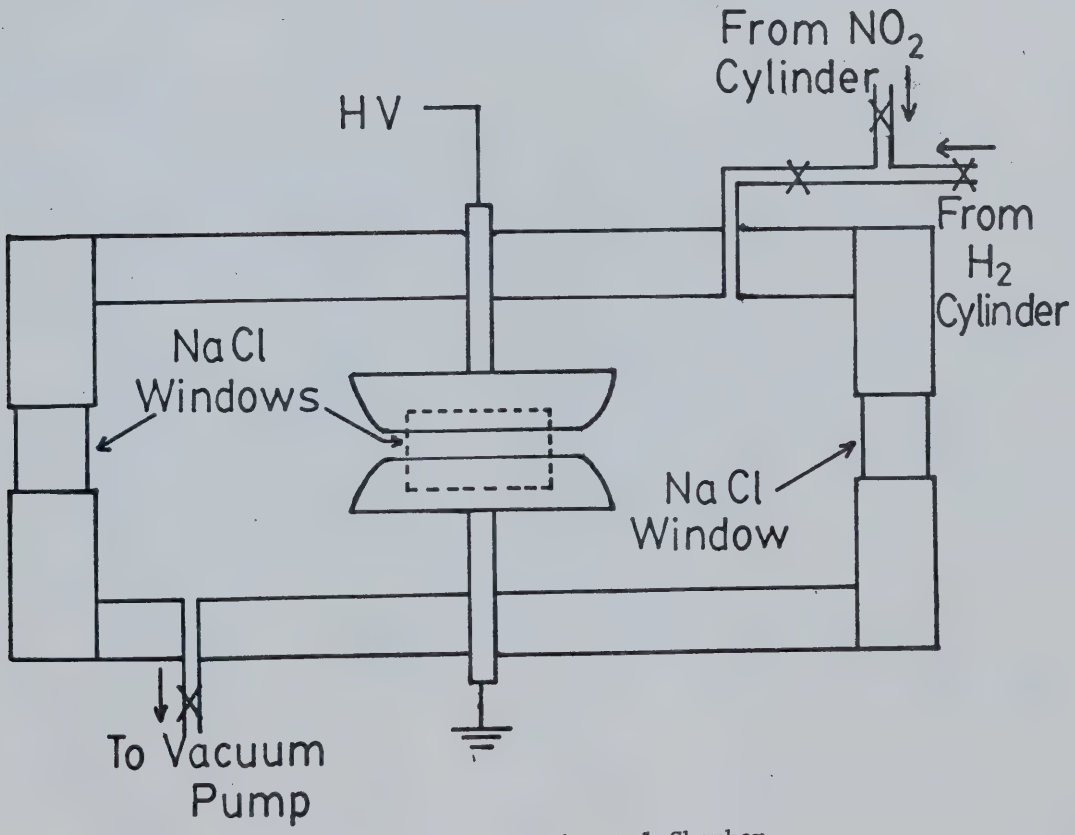

Figure 3.3 Enlarged View of Experimental Chamber

only a sample of the fluorescence radiation was monitored.

The output signal from the photomultiplier was measured for various pressures of NO_2 and NO_2-H_2 mixtures.

Care was taken to ensure that throughout the experiment the power output from the laser and the relative positions of the chamber, detector and the laser remained constant. This was done by maximizing the power output (200 mW) from the laser and adjusting the chopper position (when necessary) to get 45 mW average power transmitted past it and by keeping the detector flush against the exit window of the test chamber. The detector's position was fine adjusted by maximizing the output signal from it for a given pressure of NO_2 (6.8 torr).

3.2 Results

Figures 3.4, 3.5 and 3.6 show some typical results for the self quenching experiment at low pressures. These show the increasing intensity of fluorescence with pressure at low pressures. (See also Figure 3.10).

Figures 3.7, 3.8 and 3.9 show the decrease in intensity with increasing pressure at higher pressures. For this experiment it was observed that the maximum fluorescence intensity, about 1.2 volts, (measured at the output of the detector) was constant between about 2 to 7 torr. (See Figure 3.10a).

The amount of scattered radiation picked up by the detector was negligible as is seen from Figure 3.12 which was taken with the test chamber evacuated.

Figures 3.11, 3.13, 3.14 and 3.15 show the quenching of NO_2 meta-

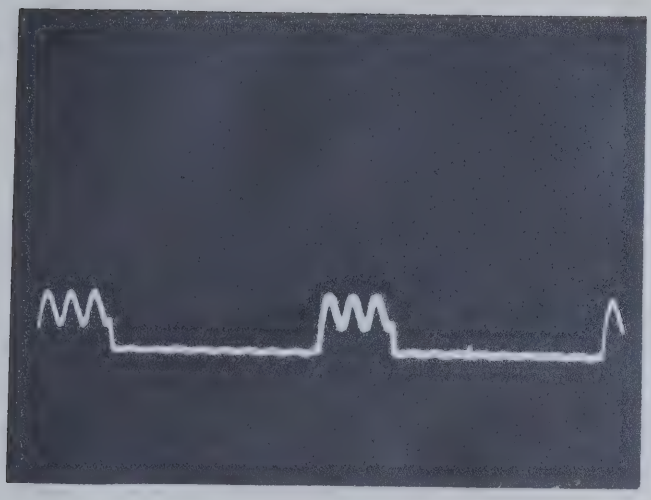

20 ms/cm

0·2 V/cm

FIG 3·4 PHOTOMULTIPLIER SIGNAL
NO_2, 0·04 TORR

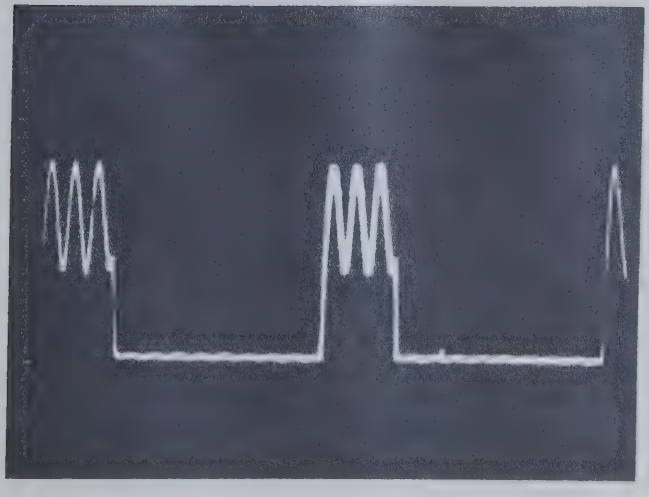

FIG 3·5 NO_2, 0·45 TORR

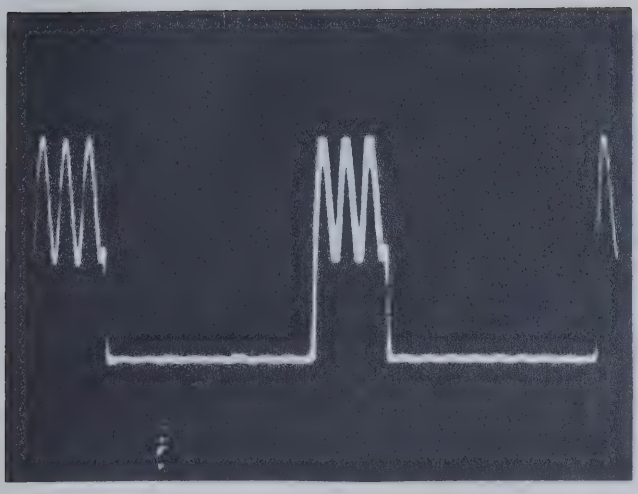

20 ms/cm
0·2 V/cm

FIG 3·6 NO_2, 2·3 TORR

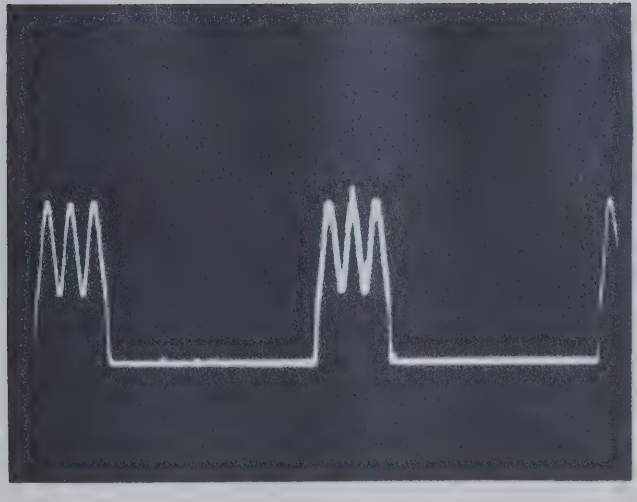

20 ms/cm
0·5 V/cm

FIG 3·7 NO_2, 9 TORR

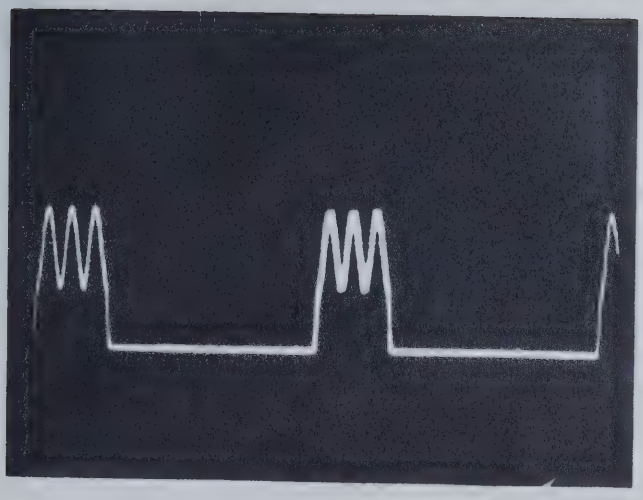

20 ms/cm
0·5 V/cm

FIG 3·8 NO_2, 12 TORR

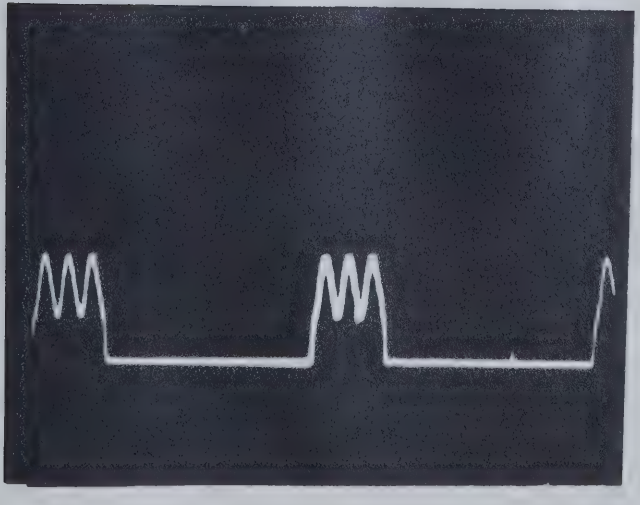

20 ms/cm
0·5 V/cm

FIG 3·9 NO_2, 16 TORR

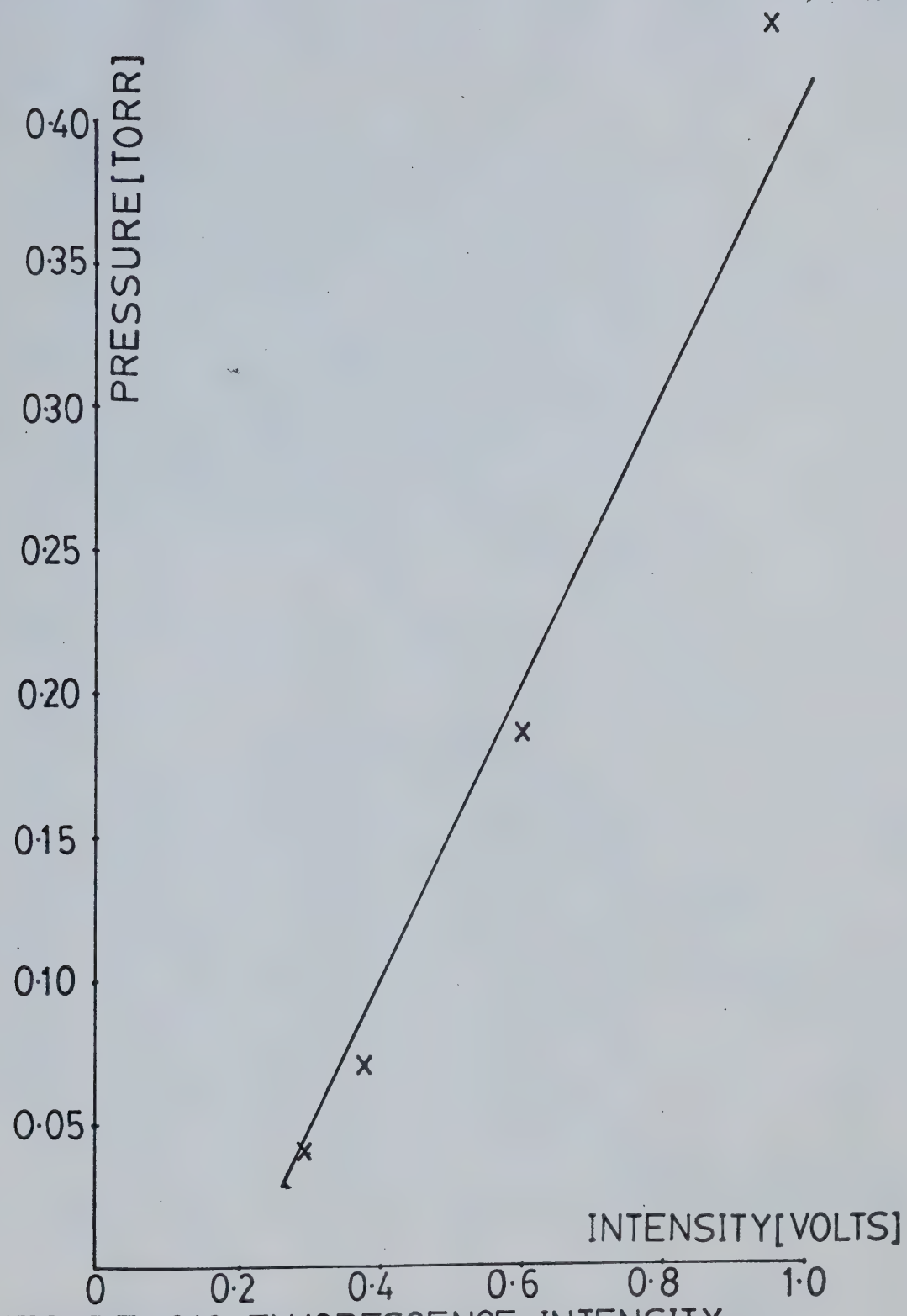

FIGURE 3·10: FLUORESCENCE INTENSITY VS. PRESSURE OF NO_2

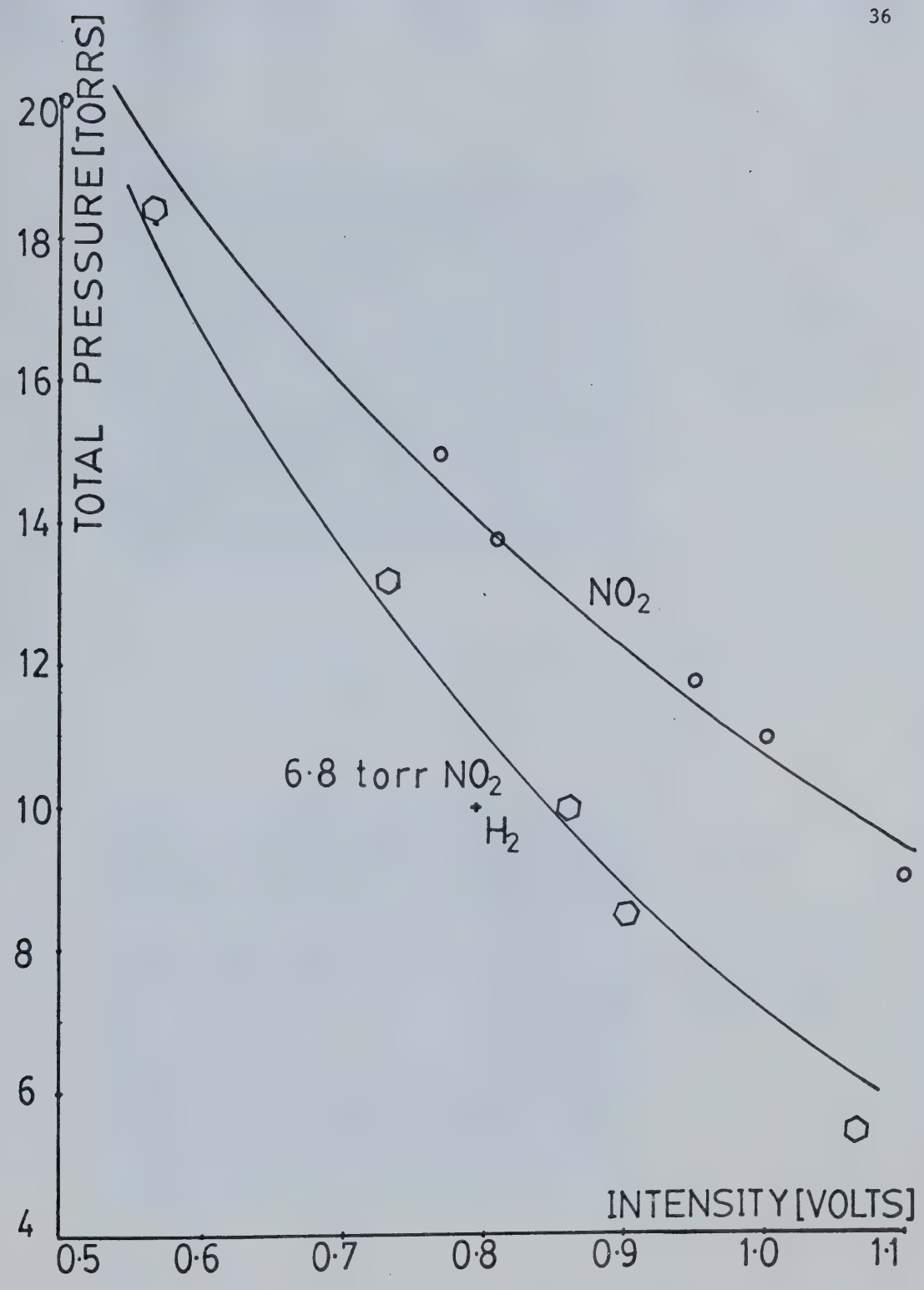

FIG·3·10$_a$: QUENCHING OF NO_2 FLUORESCENCE

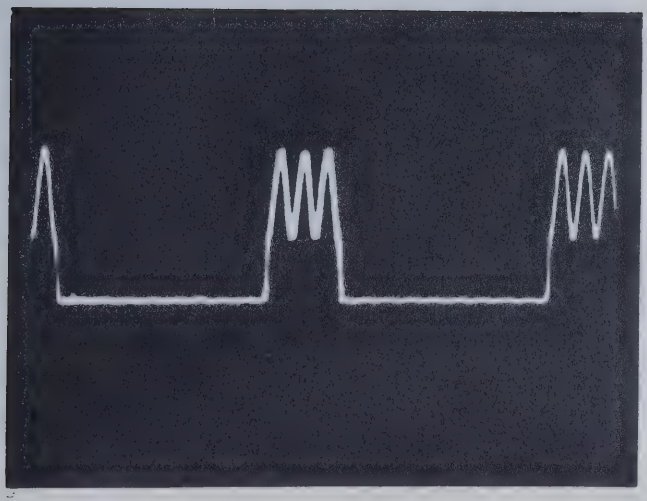

20ms/cm

0·5 V/cm

FIG 3·11 PHOTOMULTIPLIER SIGNAL
6·8 TORR NO_2, 1·2 TORR H_2.

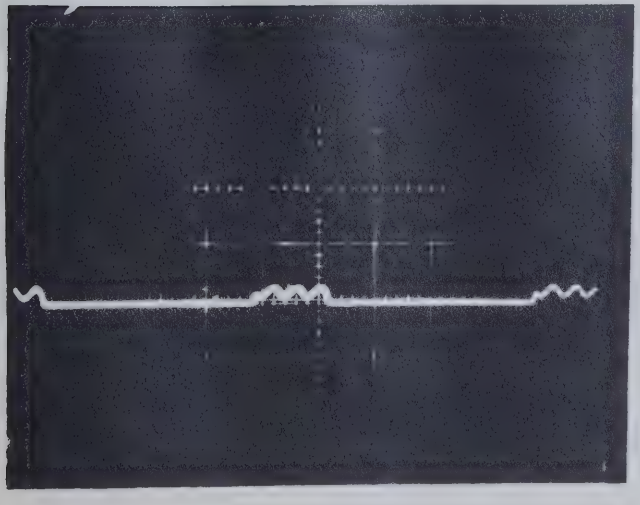

20 ms/cm

0·5 V/cm

FIG 3·12 Signal due to Stray
Radiation [Chamber Evacuated]

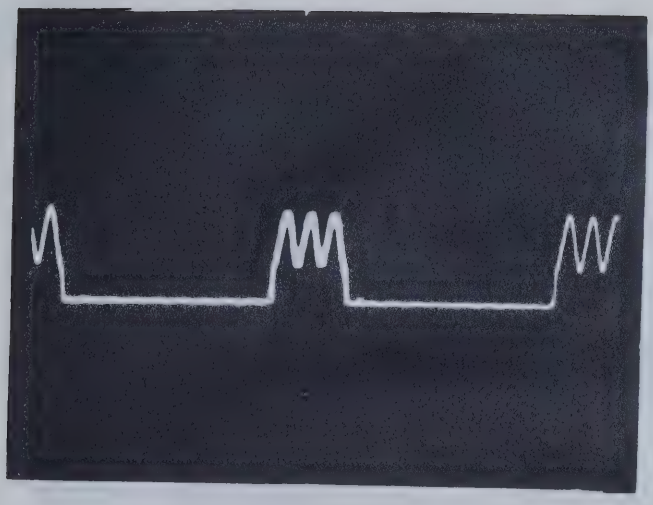

FIG 3·13 6·8 TORR NO_2, 11·7 TORR H_2.

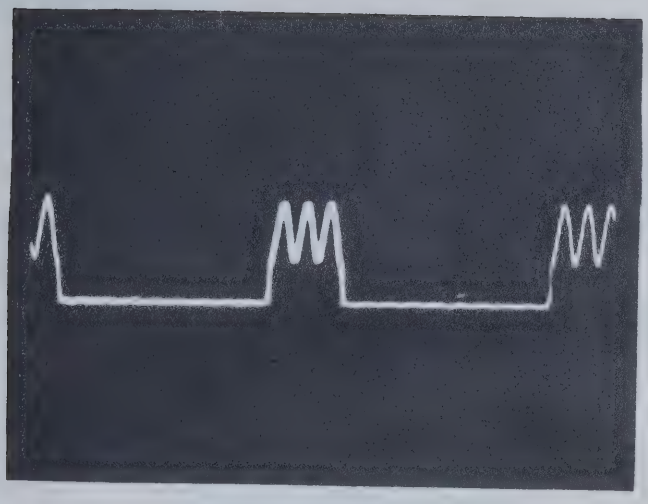

FIG 3·14 6·8 TORR NO_2, 8·7 TORR H_2

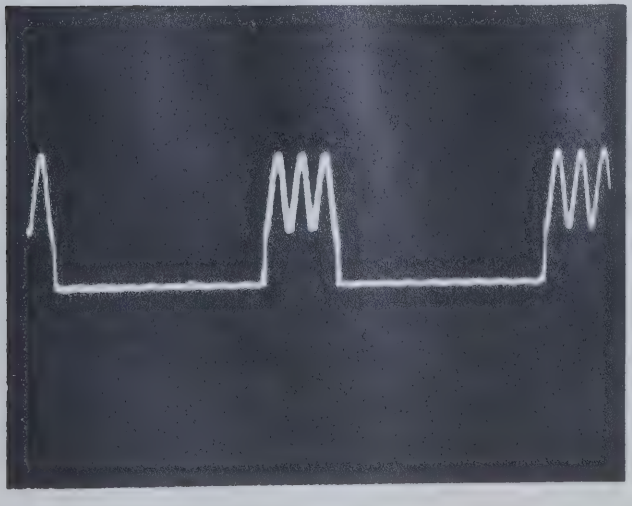

FIG 3·15 6·8 TORR NO_2, 6 TORR H_2

stable states by H_2.

3.3 Calculations

Figure 3.16 shows a simplified energy level diagram of the NO_2 molecule with the metastable electronic states lumped together.

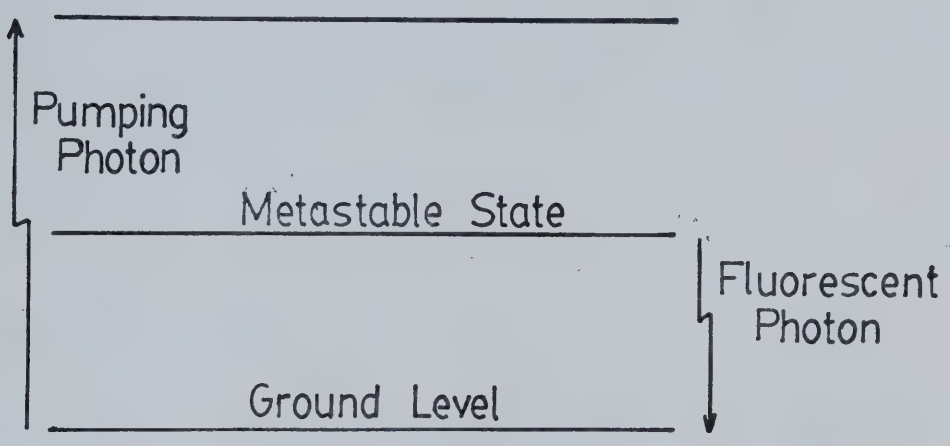

Figure 3.16 Simplified Energy Level Diagram for NO_2

Since the on-off time of the chopper was of the order of milliseconds and since the longest lived metastable state of NO_2 has a lifetime of about 70μs, steady state conditions can be assumed in each on-off cycle.

We may therefore write

$$\frac{dN^*}{dt} = 0 = R - K_1 N^* N - \frac{N^*}{\tau} \qquad (3.1)$$

where

N^* is the density of the metastable state $[cm^{-3}]$

R is the pumping rate of this state [cm^{-3} sec^{-1}]

N is the density of the unexcited molecules of NO_2 [cm^{-3}]

K_1 is the rate constant for the deactivation collision process [$cm^3 sec^{-1}$]

τ is the average lifetime of the metastable state [sec.]

In writing (3.1) the assumption that the other electronic states of NO_2 have lifetimes which are negligible in comparison to the metastable lifetime has been made. Furthermore, deactivation by other processes(like collision with walls) has been neglected. Equation (3.1) is relevant for the self quenching process.

From (3.1) it follows that

$$\frac{N^*}{\tau} = \frac{1}{\tau} \frac{R}{(K_1 N + \frac{1}{\tau})} \qquad (3.2)$$

At low pressures the pumping rate R is approximately proportional to the pressure of NO_2. Hence R is proportional to N at low pressures. Since the fluorescence intensity is proportional to $\frac{N^*}{\tau}$ it is seen from (3.2) that at low pressures I_f is proportional to N.

Hence, at low pressures, the fluorescent intensity is proportional to pressure. This is the result obtained experimentally as indicated in Figure 3.10.

Self Quenching Cross-Section

From (3.2)

$$I_f = C \frac{N^*}{\tau} = C \frac{1}{\tau} \frac{R}{(K_1 N + \frac{1}{\tau})} \qquad (3.3)$$

where C is a proportionality constant dependant on experimental conditions (e.g. geometry, detector sensitivity and oscillator strength of the NO_2 metastable states) C would have units of [Joule sec cm].

At low pressures the pumping rate R would be approximately proportional to the concentration N and hence to $\frac{P_{NO_2}}{KT}$, where T is the gas temperature and K the gas constant. Therefore

$$I_f = \frac{CK_2(P_{NO_2}/KT)}{K_1(P_{NO_2}/KT) + (1/\tau)} \cdot \frac{1}{\tau} \qquad (3.4)$$

Where K_2 is another proportionality constant.

Hence the initial slope of I_f vs P_{NO_2} (Figure 3.10), m is given by

$$m \simeq \frac{CK_2}{KT} \quad [J\ cm^{-2}\ torr^{-1}] \qquad (3.5)$$

Further the "saturation" value of I_f is given by

$$I_f = \frac{CK_2}{K_1} \cdot \frac{1}{\tau} \quad [J\ cm^{-2}] \qquad (3.6)$$

If S is the sensitivity of the detector in [J cm^{-2} $volt^{-1}$] then from equations (3.5) and (3.6) and Figures (3.10) and (3.11) we get

$$\frac{CK_2}{KT} = S \quad \text{and} \quad \frac{CK_2}{K_1\tau} = 1.2S$$

Hence, $K_1\tau = \frac{KT}{1.2}$, from which by using $\tau = 70\mu s$ [35], $T \simeq 300°K$, $K = 1.38 \times 10^{-16}$ erg/°K $= 1.03 \times 10^{-19}$ torr cm^3/°K, we obtain for K_1 the value

$$K_1 = 3 \times 10^{-13} \text{ cm}^3 \text{ sec}^{-1}$$

Converting this into an effective cross-section σ, by using [28]

$K_1 = \bar{v}\sigma$ where $\bar{v}$ is the average molecular velocity at the temperature under consideration we obtain

$$\sigma = 1.5(\mathring{A})^2.$$

This compares well with the value of $0.9(\mathring{A})^2$ quoted by Sakurai and Broida [40].

Cross-Section for Deactivation of NO_2 by H_2

If quenching by H_2 is incorporated into equation (3.1) the following equation is obtained for steady state conditions

$$\frac{dN^*}{dt} = 0 = R - K_1N^*N - K_3N^*H - \frac{N^*}{\tau} \qquad (3.7)$$

where

K_3 is the rate constant for deactivation by H_2-NO_2 collisions $[\text{cm}^3 \text{ sec}^{-1}]$ and

H is the Hydrogen density $[\text{cm}^{-3}]$.

Equation (3.7) may be re-written as follows

$$\frac{N^*}{\tau} = \frac{R}{\tau} \cdot \frac{1}{\frac{1}{\tau} + K_3H + K_1N}$$

or

$$\frac{N^*}{\tau} = \frac{R}{1 + K_3 H\tau + K_1 N\tau} \qquad (3.8)$$

which is the Stern-Volmer relationship [41]. Hence

$$\frac{I_{H'}}{I_{H''}} = \frac{1 + K_3\tau(P_{H''}/KT) + K_1\tau(P_N/KT)}{1 + K_3\tau(P_{H'}/KT) + K_1\tau(P_N/KT)} \qquad (3.9)$$

where

$I_{H'}$, $I_{H''}$ are the fluorescent intensities in mixtures in which the Hydrogen partial pressures are $P_{H'}$ and $P_{H''}$, respectively,

P_N is the partial pressure of NO_2 in the mixture.

From Figure 3.11 (using intensity values at P_H = 10 torr, P_H = 13 torr and the value of K_1 obtained above) we find the following value for K_3

$$K_3 = 8 \times 10^{-13} \text{ cm}^3 \text{ sec}^{-1}$$

which corresponds to a cross-section value of 0.9 $(\mathring{A})^2$

3.4 E-V Transfer in H_2-NO_2 Mixtures

To see if vibrational excitation of H_2 occurred in collisions with electronically excited NO_2 molecules mixtures containing up to 60 p.s.i. (about 4 atmospheres) of H_2 with about 10 torr of NO_2 were used. A d.c. electric field of about 10 KV was applied to the electrodes.

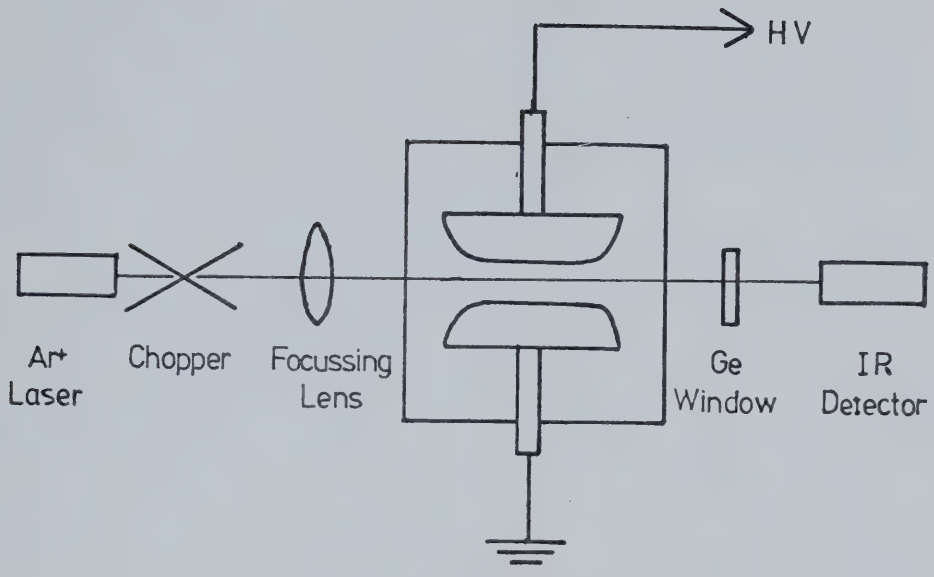

Figure 3.17 Experimental Arrangement

Vibrational excitation of H_2 would have been proved if IR radiation were detected. This method of detection of vibrational excitation has been used successfully by Polanyi and coworkers [42, 43,44] for Hg-CO and Hg-NO systems.

Since H_2 does not have a permanent dipole moment it does not exhibit an IR vibrational-rotational spectrum under ordinary conditions. This was the reason for using high gas pressures and electric fields in the above experiment since under these conditions an induced dipole moment could be expected. No IR radiation was observed.

3.5 Discussion

E-V transfer from electronically excited NO_2 to H_2 is not an efficient process inspite of the near resonant match with two of the vibrational levels of Hydrogen. It seems that the quenching of NO_2 observed occurs via an E-T transfer process.

The results of the above experiment favour the observation that there is generally no systematic variation of quenching cross-section with the resonant defect [45]. Dickens *et al* [38] have shown that E-V transfer, although exhibiting a resonant effect under certain conditions (parallel potential curves), would still be highly inefficient for processes involving excitation of more than one vibrational quantum. This is a result of the extremely small value of the matrix elements corresponding to a multiquantum jump. They further conclude that efficient transfer may be expected when crossing or near crossing of potential curves occurs.

The present evidence favours the suggestion that efficient E-V transfer occurs when a transition activated complex is formed before the products. (This will be elaborated upon in the following chapter) It appears that a chemical interaction between the reactants, strong enough to form a loosely bonded complex in the region of crossing, enhances the vibrational energy content of the products considerably [42,43].

For the system investigated (NO_2-H_2) such a complex, if it were to be formed, would necessarily have to be a five atom molecule. It is unlikely that such a complex could exist under the conditions in which the experiment was conducted.

The Landau-Teller model for V-V and V-T transfer [46] in which the probability of vibrational transition increases as the ratio of the vibrational time period to the interaction time and in which the resonance effect is pronounced, is not accurate for the E-V transfer process. The activated complex theory requires that the complex have a lifetime of at least a few vibrational periods to allow mixing of the electronic and vibrational wave functions to occur.

Nonresonant E-V transfer from the point of view of the statistical mechanical theories of Chemical Kinetics is considered in the next chapter.

CHAPTER IV

NON RESONANT ELECTRONIC TO VIBRATIONAL TRANSFER

Optical pumping appears to be the most promising method of obtaining population inversion in gases like H_2 which do not yield to the electric discharge or the electron beam methods. This is all the more so since to obtain a tunable infrared laser using a homonuclear diatomic (or a diatomic having a small dipole moment, like HD) it would be necessary to operate the laser at high pressures, as explained previously.

Resonant E-V transfer has been successfully utilized by Pettersen, Wittig and Leone [47, 48, 49] to obtain lasing action in several polyatomic gases. They produced the low lying $Br(4^2P_{1/2})$ state, which has an energy of 3685 cm^{-1}, by flash photolyzing Br_2. This energy level matches roughly with the vibrational levels of several polyatomic molecules; CO_2 (101, 021) N_2O (140), HCN (120, 050) and C_2H_2 (01002). This electronic state also corresponds to the first vibrational level of H_2 (about 4000 cm^{-1}), but the method cannot be used to obtain an infrared H_2 laser since a chemical reaction occurs in a mixture of H_2 and Br_2 yielding HBr [50, 51, 55].

Fortunately, a resonant match between the levels is not an essential prerequisite in many other efficient E-V transfer processes. Such processes have long been known to occur [52, 53, 54]. Here, efficient conversion of electronic to vibrational energy occurs essentially because of a mixing of the wavefunctions representing these types of energies. A loosely bonded activated complex molecule is formed which then dissociates into vibrationally excited products.

The Activated Complex Theory of chemical kinetics, and its extension by Rice, Ramsperger, Kassel and Marcus (the RRKM Theory) are general theories which apply to many chemical processes in which energy redistribution occurs [56-59]. Some processes like the quenching of electronically excited oxygen (O^1D) atoms by N_2 in which no new chemical products are formed can also be treated by this theory [60].

For reactions on which enough data are available, the RRKM Theory allows a quantitative estimation of the amounts of vibrational and translational energy content in the products. For instance, Tully [60] has, by an extension of the RRKM Theory, successfully explained the large cross-section in the quenching of $O(^1D)$ by N_2;

$$O(^1D) + N_2 \rightarrow O(^3D) + N_2 + \Delta E$$

This Chapter is divided into three main parts. Section 1 examines the activated complex and the RRKM Theories. Some relevant background material is also presented. In Section 2, a calculation for the cross-section of quenching in the $Na(^2P) + H_2 \rightarrow Na(^2S) + H_2 + \Delta E$ reaction is given, together with the (partial)cross-section for the excitation of the second vibrational level of H_2.

Finally, the E-V transfer process is viewed in terms of the breakdown of the Born-Oppenheimer Approximation. It is noted that under these conditions, since the electronic and nuclear (vibrational and rotational) motions are no longer separable, efficient E-V transfer may be expected. From this point of view, the necessity of a loosely bonded activated complex [54] and non-parallel potential curves [39, 63] follow automatically.

The conditions under which the Born-Oppenheimer Approximation breaks down can also be used as a basis for selecting atoms (or molecules) which would pump (by E-V transfer) a potential laser molecule. A general criterion for this choice is presented.

4.1 Chemical Kinetics [56, 57, 58]

It must be noted that there exists a great deal of confusion in the current literature regarding notation in this field. Robinson and Holbrook [57] have attempted to rectify the situation by defining a consistent set of symbols and comparing them with those of other workers. Unless otherwise stated, their notation will be followed here (see Appendix V).

Consider a reaction of the following type

$$D + (B - C) \rightarrow (D - B) + C \qquad (4.1)$$

in which a diatomic molecule B-C reacts with an atom D yielding D-B and the atom C.

Many such reactions can be analyzed in terms of a potential energy diagram like the one shown in Figure 4.1.

The reaction path shown in Figure 4.1 is the path of minimum energy and is hence the most probable one followed. The "saddle point" or the col shown on this path has the highest energy *on the reaction path.* Any other path would have a maximum at a higher energy level than the saddle point.

A section through the reaction path is shown in Figure 4.2.

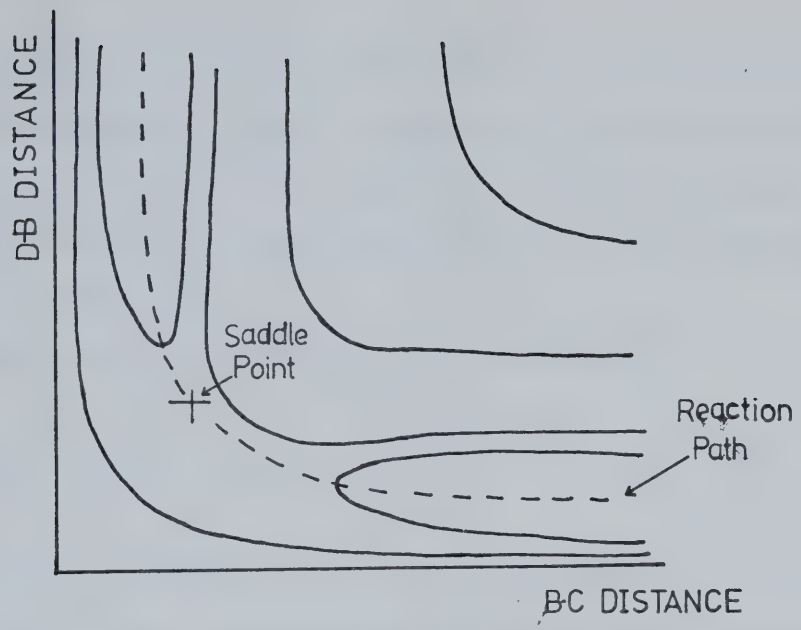

Figure 4.1 A "typical" potential energy surface diagram

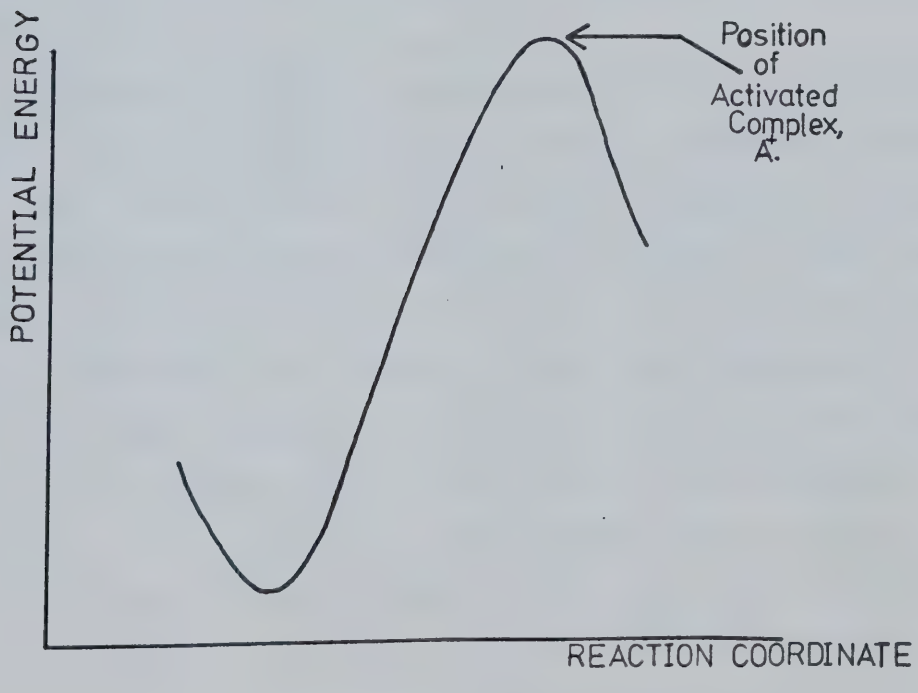

Figure 4.2 Section through a reaction path

The Activated Complex Theory also known as the Absolute Rate Theory and the Transition State Theory, postulates that a loosely bonded molecule exists around the region of the highest point in the reaction path. This molecule is called the activated complex and is in equilibrium with the 'reactants', D and B-C.

Hence, equation (4.1) is more accurately written as

$$D + (B - C) \rightleftarrows D \cdot\cdot B - C \rightarrow (D - B) + C \qquad (4.2)$$

The theory stipulates that all the activated complexes dissociate into products. Hence, although the probability of an activated complex being formed is, in general not unity, once it is formed the Activated Complex Theory assumes that the probability of passage over the potential barrier is unity.

Recent work (theoretical and experimental) has shown that, in general, the reacting particles form an "Energised" Molecule (collectively denoted by A^*) which has enough energy to dissociate into the products. However, A^* is distinct from the Activated Complex in that although the former has enough energy, the distribution of this energy may not be conducive to an immediate dissociation into products. It is only after this molecule takes on the right configuration, in which the energy is favourably distributed in its different degrees of freedom, that the reaction goes to completion. For this reason, some authors prefer to call the Activated Complex by the term "Critical Configuration" [59, 60]. (In our notation the Activated Complex will be denoted by A^+).

Equation (4.2) represents a chemical reaction. However, the Activated Complex Theory applies to many processes, in which only the energy in participating particles is redistributed and which cannot strictly be called chemical reactions. An important group of such processes that can, nonetheless be treated by the Activated Complex Theory and its more accurate extension - the RRKM Theory - is the quenching of electronically excited atoms by diatomic or polyatomic molecules.

The existence of activated complexes has been proven experimentally in many instances [61]. Furthermore, the concept of a reaction path easily explains why for certain reactions the products take up most of the energy of exothermicity as translational energy, whereas, in others, the conversion is essentially into vibration. This is illustrated in Figures 4.3 and 4.4.

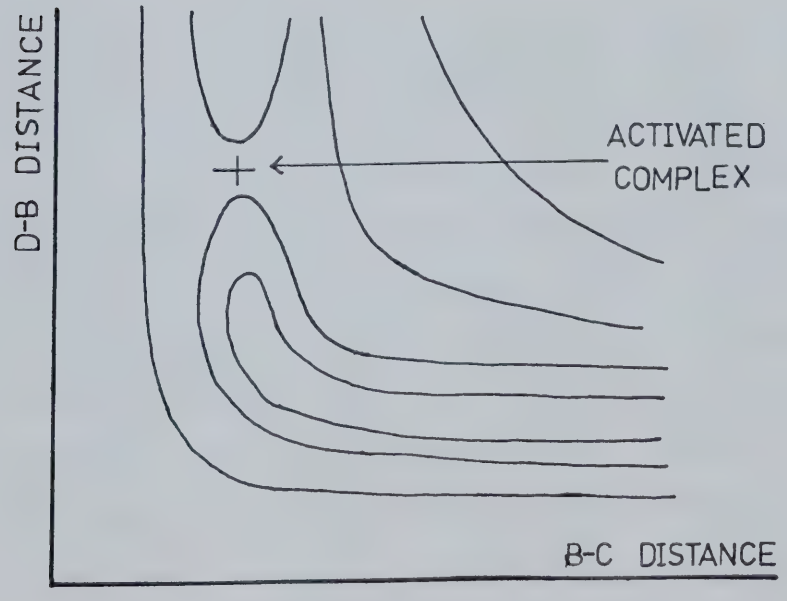

Figure 4.3 A potential energy surface of the "attractive" type, for the reaction D+BC→DB+C [56]

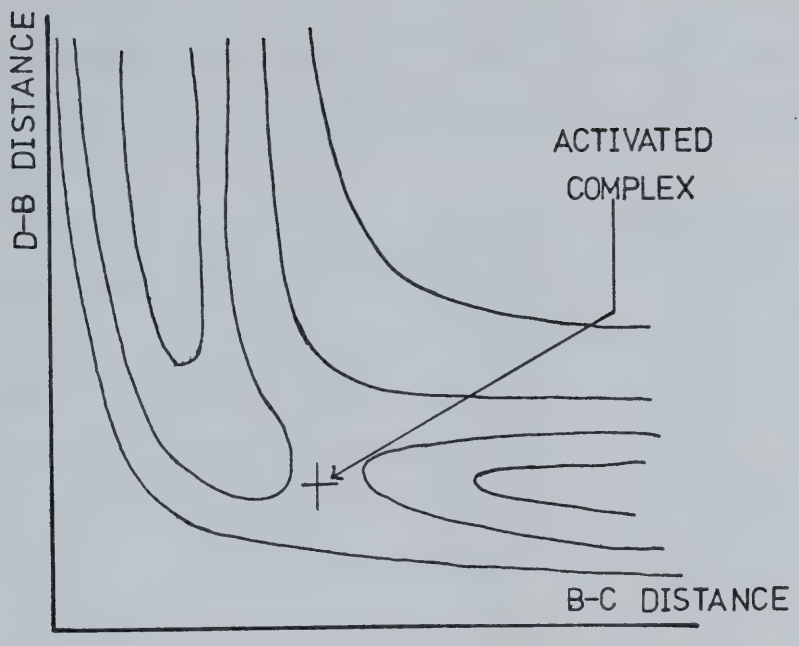

Figure 4.4 A potential energy surtace of the "repulsive" type, for the reaction D+BC→DB+C [56]

Figure 4.3 illustrates the type of reaction where the molecule DB might be expected to take up most of the energy released in the form of vibration since the activated complex occurs at a position where the D-B bond is stretched. Such a potential energy surface is sometimes called the "attractive type" as opposed to the "repulsive type" shown in Figure 4.4. In the latter, the activated complex occurs at relatively large distances of C from DB. Hence, most of the energy released goes into translational kinetic energy of the products. In general, the potential energy curves are such that the products absorb the energy of reaction in both these modes although the distribution is usually uneven.

Quenching reactions are quite similar although no new chemical products

occur. Quenching may be expected to produce either vibrational or translational energy depending on the energy distribution at the critical configuration.

The potential energy surface concept holds, in principle, for any activated complex. An N-atom complex molecule has 3N-6 vibrational degrees of freedom if it is nonlinear and 3N-5 vibrational degrees of freedom if linear [62]. Hence, a complete potential energy plot for such a molecule would be an n dimensional plot (where n = 3N - 6 or 3N - 5). This being hard to draw, the procedure is to hold some of the coordinates fixed and depict the variation of potential energy with the rest of the coordinates. Hence, Figures 4.3 and 4.4 are valid plots for a nonlinear triatomic system with the angle between its two bonds fixed. It could also represent the plot for a linear triatomic with the two bending vibrations' normal coordinates held fixed [57].

(It might also be pointed out that whenever a potential energy diagram for a molecule is plotted,it is implied that the vibrational motion of the molecule takes place under the influence of this potential, for a given electronic state [18]. This, in turn, implies that the nuclear and electronic motions of the molecule can be separated by the Born-Oppenheimer Approximation. Under the condition when this approximation is not accurate, the potential energy surface concept, strictly speaking, does not hold [18]).

Consider the process indicated by (4.2). The activated complex theory makes the hypothesis that the activated complex (D ···B-C) which we will denote by A^{+}, is in equilibrium with the reactants D and B-C even when the reactants and the products are not in equilibrium amongst themselves [56]. Under these conditions, statistical mechanical theory [56, 57] leads to

the following expression for the overall rate constant k

$$k = \frac{-\frac{d}{dt}[D]}{[D][BC]} = \frac{KT}{h} \frac{Q^+}{Q_D Q_{BC}} \exp(-E_o/KT) \qquad (4.3)$$

where Q^+, Q_D, Q_{BC} are the partition functions of the activated complex, the atom D and the molecule BC (in evaluating Q^+, the activated complex is considered to have one less degree of freedom than would be normally expected, since the derivation of equation (4.3) treats the motion of the complex over the potential barrier as a degree separate from the others; the effect of this is expressed by the factor $\frac{KT}{h}$ in the above equation).

E_o is the difference between the zero point energies of the activated complex and the reactants, which may be regarded as the activation energy for the reaction at the absolute zero of temperature (see also Figure 4.5).

k and h are the Boltzman and Planck constants respectively, and

T is the absolute temperature (See Appendices V and VI)

The Activated Complex Theory has been successful in explaining reaction rates for many processes. At low pressures however, there is a substantial discrepancy between the experimental rates observed and the theoretical ones predicted.

The RRKM Theory is an extension of the activated complex which has found the most success from amongst present day theories. It postulates the existence of an energized molecule *before* the activated complex is formed. The Activated Complex Theory, on the other hand, does not distinguish between these two states.

Before going into the mathematical formulation of the RRKM Theory, it might be useful to clarify some of the terminology commonly employed. For this we refer to Figure 4.5 and to Appendix 5.

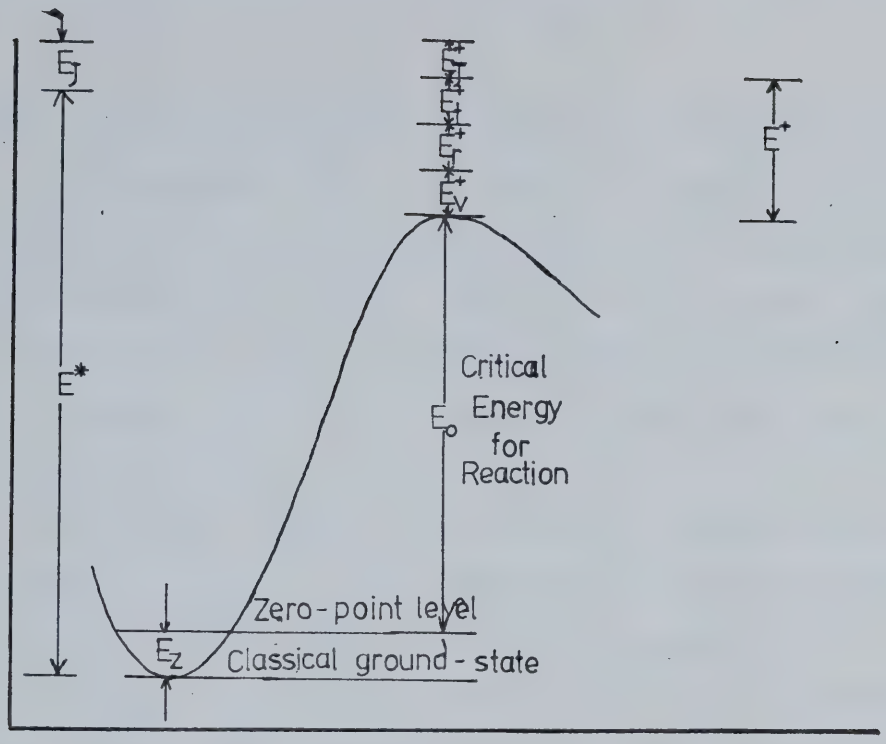

Figure 4.5 Energy level diagram relevant to the RRKM treatment [56,57]

An energy mode is said to be *adiabatic* if it stays in the same quantum state during the reaction. Generally, an adiabatic mode has the same energy content throughout the reaction. However, this may not be true for an adiabatic rotational mode since in many instances the configuration of the system and hence its moment of inertia changes considerably during a reaction. Hence, although the rotational state may be characterized by the same quantum numbers, its energy content might change.

Adiabatic rotations are denoted by E_J and E_J^+ in Figure 4.5.

Any form of energy which cannot be redistributed is called *fixed energy*. Examples of fixed energies are the zero point levels of molecular vibrations, E_z and E_o in Figure 4.5.

The RRKM Theory as normally applied assumes that all nonadiabatic degrees of freedom can take part in the redistribution of energy in the

various modes of the system and are hence called also *active modes*.

An *energized molecule*, A^*, is defined as a molecule which contains, in its active degrees of freedom, a nonfixed energy E^* greater than E_o (the difference between the zero point levels of the reactant's and the activated complex). E_o is the activation energy of the reaction at absolute zero of temperature and is hence, classically, the critical value of E^* below which reaction cannot occur.

The *activated complex* is a species having a configuration corresponding to a position at the top of the energy barrier in the reaction path.

The total active energy in the energized molecule denoted by E^*, can be resolved into a vibrational component, E_v^* and a rotary component, E_r^*.

$$E^* \equiv E_{vr}^* = E_v^* + E_r^*$$

Similarly the total active energy in an activated complex is defined as E^+.

$$E^+ = E_v^+ + E_r^+ + E_t^+$$

where

E_v^+, E_r^+ and E_t^+ are the vibrational, rotational and translational (along the reaction coordinate) components of E^+.

The RRKM reaction scheme is

$$A + M \underset{k_2}{\overset{\delta k_1(E^* \to E^* + \delta E^*)}{\rightleftharpoons}} A^*_{(E^* \to E^* + \delta E^*)} + M \qquad (4.4a)$$

$$A^*_{(E^*)} \xrightarrow{k_a(E^*)} A^+ \qquad (4.4b)$$

$$A^+ \xrightarrow{k^+(E_t^+)} \text{products} \qquad (4.4c)$$

Equation (4.4a) denotes the formation and deactivation of energized molecules A^*.

Equations (4.4b) and (4.4c) show the formation and dissociation of the complexes (A^+), respectively.

k_1, k_a and k^+ are functions of the corresponding energies, this being another major difference between the RRKM and Activated Complex Theories.

$\delta k_{1(E^* \to E^* + \delta E^*)}$ is the rate constant for the reaction which produces energized molecules having energies between E^* and $E^* + \delta E^*$.

Applying the steady state condition to reactions (4.4a) and (4.4b) we obtain the following equation, in which square brackets denote the concentration of the appropriate species,

$$0 = \frac{d[A^*]}{dt} = \delta k_1[A][M] - k_2[A^*][M] - k_a(E^*)[A^*] \qquad (4.5)$$

(The subscripts ($E^* \to E^* + \delta E^*$) have been dropped from equation (4.5) for convenience. Hence,

$$[A^*] = \frac{\delta k_1[A]/k_2}{1 + k_a(E^*)/k_2[M]} \qquad (4.6)$$

The overall rate of reaction (formation of activated complexes - which is the rate at which particles arrive at the critical configuration) is

$$k_a(E^*)[A^*] = \frac{k_a(E^*)\,\delta k_1/k_2[A]}{1 + k_a(E^*)/k_2[M]} \qquad (4.7)$$

The unimolecular rate constant for the process is defined by the following equation

$$k_{uni} = \frac{1}{[A]}\left(\frac{-d[A]}{dt}\right)$$

or

$$-\frac{d[A]}{dt} = k_{uni}[A] \qquad (4.8)$$

From equations (4.7) and (4.8) the overall unimolecular rate constant for the processes denoted by equations (4.4a) to (4.4c) is given by

$$k_{uni} = \int_{E^*=E_o}^{\infty} \frac{k_a(E^*)/k_2}{1 + k_a(E^*)/k_2[M]}\, dk_1(E^* \rightarrow E^* + dE^*) \qquad (4.9)$$

The lower limit in the integral is E_o because this is the difference between the zero point levels of the reactants and activated complex molecules and hence is the minimum energy required for the formation of the latter.

To evaluate (4.9), we need an expression for $k_a(E^*)$, the rate constant for the formation of activated complexes from energized molecules having active energy E^*. This expression is also fundamental to any analysis of the vibrational energy of the products in which we are interested. (This will be seen below in Section 2).

In the steady state, we find from equations (4.4b) and (4.4c)

$$[A^*]k_a(E^*) = k^+(E_t^+)[\vec{A}^+] \qquad (4.10)$$

where $\vec{A}^+$ denotes the activated complexes moving in the forward direction (towards dissociation into products)only, over the saddle point in the reaction path. In most cases [57] it can be shown that to a good approximation

$$[\vec{A}^+] = \frac{1}{2}[A^+]$$

where $[A^+]$ is the total concentration (including complexes moving in both directions).

Hence

$$k_a(E^*) = \frac{1}{2} k^+(E_t^+) \frac{[A^+]}{[A^*]} \qquad (4.11)$$

Since the active energy of a complex can be divided, in different ways, into the energy of vibration and rotation (E_{vr}^+) and the energy of translation in the reaction coordinate (E_t^+), the processes denoted by (4.4b) and (4.4c) can, in effect, be resolved into those represented by (4.4d) below.

$$A^*(E^*) \xrightarrow{k_a(E_{vr}^+, E_t^+)} A^+(E_{vr}^+, E_t^+) \xrightarrow{k^+(E_t^+)} \text{Products} \qquad (4.4d)$$

where we have used the fact that

$$E^* = E^+ + E_o$$

The rate constant $k_a(E^*)$ can hence be written in the more general form

$$k_a(E^*) = \sum_{E_{vr}^+=0}^{E^+} \frac{1}{2} k^+(E_t^+) \frac{[A^+_{(E_{vr}^+, E_t^+)}]}{[A^*_{(E^*)}]} \qquad (4.12)$$

To find $k^+(E_t^+)$, the decomposition of the complex into products may be treated as the translation of a particle of mass μ in a one-dimensional box of length δ, where the latter is an arbitrary (small) region at the top of the energy barrier which may be said to define the activated complex.

(We note that the final expression for $k_a(E^*)$ is independent of both μ and δ. See below). The speed of translation is $(2E_t^+/\mu)^{1/2}$ and the time taken to cross the barrier is hence $\delta/(2\ E_t^+/\mu)^{1/2}$. The rate constant is the inverse of this quantity

$$k^+(E_t^+) = (2E_t^+/\mu\delta^2)^{1/2} \qquad (4.13)$$

The ratio $[A^+_{(E_{vr}^+, E_t^+)}]/[A^*_{(E^*)}]$ has to be evaluated for the derivation of $k_a(E^*)$. It should be noted that in equation (4.12) this ratio is for the values of A^+ and A^* *at equilibrium*.

Statistical mechanical considerations [57] enable us to write this ratio as a ratio of the corresponding partition functions.

Hence,

$$\left\{ \frac{A^+_{(E_{vr}^+, E_t^+)}}{A^*_{(E^*)}} \right\}_{eqm} = \frac{Q(A^+)}{Q(A^*)} = \frac{(\sum g_i^+)\exp(-E^+/KT)}{(\sum g_i^*)\exp(-E^*/KT)} \qquad (4.14)$$

where

$Q(A^+)$ and $Q(A^*)$ are the partition functions of the activated complex and the energized molecules respectively,

$\sum g_i^+$ and $\sum g_i^*$ are the number of quantum states in the energy range $E^+ + \delta E^+ = E^* + \delta E^*$

Equation (4.14) therefore reduces to

$$\left\{\frac{[A^+]}{[A^*]}\right\}_{eqm} = \frac{N^+(E_{vr}^+, E_t^+)}{N^*(E^*)} \qquad (4.15)$$

where the subscripts have been dropped for convenience.

$$N^+(E_{vr}^+, E_t^+) = N^+(E_{vr}^+, E_t^+) = P(E_{vr}^+)N_{rc}^+(E_t^+) \qquad (4.16)$$

where

$P(E_{vr}^+)$ is the number of vibrational-rotational levels of A^+ with vibrational-rotational nonfixed energy equal to E_{vr}^+

and

$N_{rc}^+(E_t^+)\delta E_t^+$ is the number of states with translational energy in the range $E_t^+ \rightarrow E_t^+ + \delta E_t^+$ [57].

Quantum mechanical treatment [65] of the translation of a particle, mass μ, in a box of length δ produces the result that the energy is quantized and n, the number of levels having energy up to and including E_t^+ is given by

$$n = \left(\frac{8\mu\delta^2 E_t^+}{h^2}\right)^{1/2} \qquad (4.17)$$

where

h is Planck's constant.

The density $N^{+}_{rc}(E^{+}_{t})$ is therefore given by

$$N^{+}_{rc}(E^{+}_{t}) = \frac{dn}{dE^{+}_{t}} = \left(\frac{2\mu\delta^2}{h^2 E^{+}_{t}}\right)^{1/2} \qquad (4.18)$$

Substituting (4.13), (4.16) and (4.18) into (4.12) the following important RRKM expression is finally obtained

$$k_a(E^*) = \frac{1}{hN^*(E^*)} \sum_{E^{+}_{vr}=o}^{E^{+}} P(E^{+}_{vr}) \qquad (4.19)$$

As might be expected, when equation (4.19) is substituted into (4.9), the RRKM expression for k_{uni} reduces to the Activated Complex Theory expression (4.3) in the high pressure limit ($[M] \to \infty$) [57].

Equation (4.19) was first derived by Marcus [59] and is the starting point in the calculation (section 2 below) for the vibrational energy content in a quenching molecule after a collision with an excited electronic species.

4.2 E-V Transfer

Many quenching processes of the type

$$D^* + AB \to D + AB(v) + \Delta E \qquad (4.1a)$$

where

D^* is an electronically excited atom,

AB(v) is a vibrationally excited molecule,

and

ΔE represents the energy defect, can be investigated by extending the RRKM treatment described above.

Tully [60] has applied the fundamental RRKM expression, equation (4.19), to the quenching of electronically excited Oxygen atoms by Nitrogen molecules:

$$O(^1D) + N_2 \rightarrow O(^3P) + N_2(v) + \Delta E \qquad (4.20)$$

The treatment developed by Tully is especially for spin forbidden reactions like (4.20). The principle, however, is general enough to be applied to other reactions too.

The RRKM theory has been particularly successful in explaining the high efficiency of the E-V transfer process in reaction (4.20) which cannot be explained otherwise. Thus, for instance, the Wigner Spin Conservation Rule predicts that a reaction like (4.20) should occur only with an extremely small probability (being "forbidden" under the Rule). However, it has been found experimentally that the reaction has one of the *highest* rates observed for any process of this type. The RRKM Theory explains this otherwise anomalous result by postulating the formation of a relatively long lived energized molecule (N_2O^*).

Equation (4.19) is rewritten to include the energy of the activated complex and the angular momentum explicitly. k_a is also assumed to be dependent on the translational energy of the complex. The equation therefore becomes

$$k_{ai}(E^+, J, E_t^+) = \frac{1}{hN^*(E^*)} \; W(E_{vr}^+) \qquad (4.19a)$$

where

E^+ is the total active energy of the complex ($E^+ = B_i^+ + E_{vr}^+ + E_t^+ = B_i^+ + E_v^+ + E_r^+ + E_t^+$; B_i being an additional form of active energy defined here as the height of the centrifugal barrier that the activated complex has to cross before dissociating into products. Note that in the usual RRKM treatment, E^+ is written as $E^+ = E_{vr}^+ + E_t^+ = E_v^+ + E_r^+ + E_t^+$. Furthermore, the subscript i is used to emphasise the fact that there may be more than one reaction path leading to the formation of an activated complex), J is the total angular momentum of the complex and $W(E_{vr}^+)$ denotes the sum $\sum_{E_{vr}^+=0}^{E^+} P(E_{vr}^+)$

Another improvement is made by assuming that all activated complexes do not necessarily decay into products as the normal RRKM theory assumes. Hence, a probability factor $\Gamma_i(E_t^+, E_{vr}^+, B_i^+)$, is included on the right hand side of equation (4.19a).

Equation (4.19a) is therefore modified to equation (4.19b)

$$k_{ai}(E^+, J, E_t^+) = \Gamma_i(E_t^+, E_{vr}^+, B_i^+) \frac{W(E_{vr}^+)}{hN^*(E^*)} \qquad (4.19b)$$

4.2.1 Quenching Cross-Sections

Equation (4.19a) may be viewed as describing the rate of *arrival* at the critical configuration, while (4.19b) describes the rate at which these activated complexes *emerge* from the critical configuration leading to products with translational energy E_t^+ along the reaction coordinate.

Γ_i is assumed to be close to unity for reaction paths not involving curve crossing. For paths that do involve crossing (or "avoided" crossing)

Γ_i is assumed to be given by the Landau-Zener [66-69] formula for transmission coefficient:

$$\Gamma_i(E_t^+, E_{vr}^+, B_i^+) \simeq \Gamma_i(E_t^+) = 1 - \exp[-A_i/(E_t^+)^{1/2}] \qquad (4.21)$$

where

A_i is the Landau-Zener coupling coefficient for the electronic transition under consideration.

Note that in equation (4.21) we have made the assumption that the dependence of Γ_i on E_t^+ is stronger than that on E_{vr}^+ and B_i^+. This seems reasonable if it is borne in mind that Γ_i reflects the probability of an electronic transition occurring at critical configurations that are defined by curve crossing.

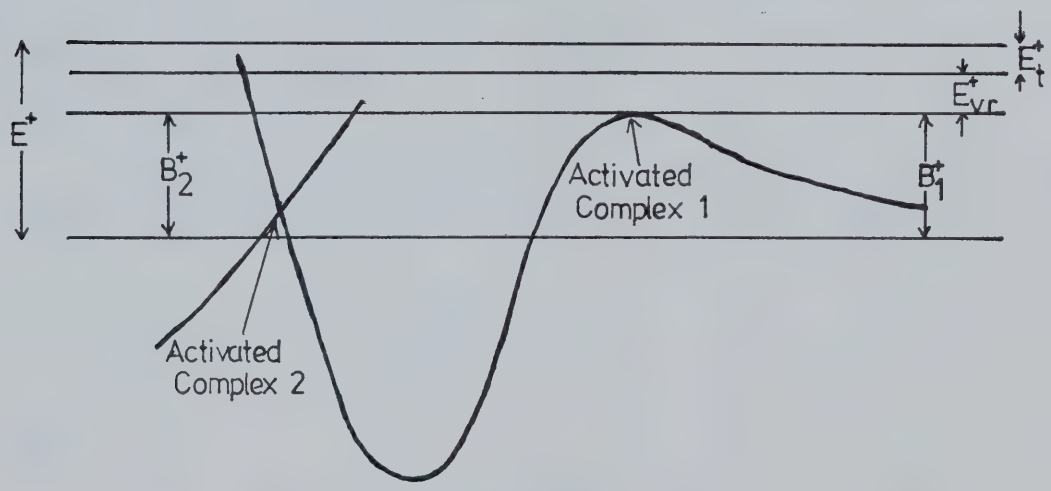

Figure 4.6 Effective potential along some arbitrary reaction coordinate illustrating the two paths by which critical configurations may be reached [60].

If $\Delta_i(E^+,J)$ is defined as

$$\Delta_i(E^+,J) = \int_0^{E^+-B_i^+(J)} k_i(E^+,J,E_t^+)dE_t^t \qquad (4.22)$$

then it follows that the probability that an activated complex, A^+, with total active energy E^+ and angular momentum J, will decay into products via channel i is given by

$$\phi_i(E^+,J) = \frac{\Delta_i(E^+,J)}{\sum_j \Delta_j(E^+,J)} \qquad (4.23)$$

where the summation is over all possible reaction paths leading to an activated complex.

The centrifugal barrier height $B_i^+(J)$ is needed in order to evaluate the definite integral in equation (4.22).

This can be found if the form of the potential energy (in Figure 4.6) around the critical configuration is known. Let this value of potential energy be denoted by V_i^+.

Around the critical configuration on the reaction path the total energy (or "the effective potential barrier") [18] will be given by

$$V_{eff}^+(J,r) = V_i^+(r) + \frac{J^2}{2\mu_i R_i^{+2}} \qquad (4.24)$$

where

μ_i is the reduced mass of the complex

R_i^+ is its effective radius

[The second term on the right hand side of (4.24) is just the kinetic energy of rotation of the complex, hence the name centrifugal

barrier for $(V_{eff})_{max} \equiv B_i(J)$].

It will be assumed that for channels not involving curve crossing the value of V_i^+ will be of the form

$$V_i^+(r) = - C\, r^{-6} \tag{4.25}$$

where

C is the van der Waal's coupling coefficient for the interacting particles,

r is the effective distance between these particles.

Using (4.25) in (4.24) differentiating with respect to r and setting $\frac{\partial v}{\partial r} = 0$ to find the maximum yields

$$(r^+)^4 = \frac{6C\mu_i}{J^2}$$

from which

$$(V_{eff})_{max} = B_i^+(J) = \frac{J^3}{(54C\mu_i^3)^{1/2}} \tag{4.26}$$

This is the value of the centrifugal potential barrier for a critical configuration not involving curve crossing.

For the critical configuration(s) involving curve crossing, equation (4.24) is used. This requires that the coordinates of the points of intersection be known reasonably accurately. (As will be seen below, this restriction usually causes difficulties since potential energy surfaces for many processes are known only very roughly, if at all).

The cross-section for the reaction occurring (to completion) via

channel i is given by

$$\sigma_i(E_c) = \sigma_{cc}(E_c) \int_0^{J_{max}} \rho(J)\ \phi_i(E^+,J)dJ \qquad (4.27)$$

where

E_c is the initial collision energy, which is a function of the translational temperature,

σ_{cc} is the cross-section for complex formation,

$\rho(J)$ is the normalized distribution of angular momentum of the complexes.

σ_{cc} can be written in the form

$$\sigma_{cc} = g_i \pi\ J^2_{max}\ (E_c)/2\mu_i E_c \qquad (4.28)$$

where

g_i is the statistical degeneracy of channel i.

This follows from the fact that the effective collision cross-section is directly proportional to the kinetic energy due to rotation and inversely proportional to the centrifugal barrier height.

To evaluate $\sigma_i(E_c)$ in equation (4.27), the values of the total number of active vibrational-rotational levels, $W(E^+_{vr}) = \sum_{E^+_{vr}=0}^{E^+} P(E^+_{vr})$ in the activated complex, and the number of energy levels of the energized molecule per unit energy, $N^*(E^*)$, have to be obtained.

This is done by treating the complex as a set of S_{eff} classical harmonic oscillators, each oscillating at a frequency ν_i [57].

The value of S_{eff} is usually taken to be

$$S_{eff} = \frac{s + r}{2} \tag{4.29}$$

where

s is the number of vibrational modes at the critical configuration,

r is the number of active rotations of the complex [57]

The following expressions result

$$W(E^{+}_{vr}) \simeq \frac{(E^{+}_{vr})^{S_{eff}}}{(S_{eff})!\ \Pi(h\nu_i)} \tag{4.30}$$

and

$$N^{*}(E^{*}) = \frac{(E^{*})^{S_{eff}-1}}{(S_{eff} - 1)!\ \Pi(h\nu_i)} \tag{4.31}$$

where

$\Pi(h\nu_i)$ is the product $\prod_{i=1}^{S_{eff}} (h\nu_i)$.

(The derivations of these expressions are given by Robinson and Holbrook in reference [57]).

If a system having only two paths leading to critical configurations is considered (path no. 2, involving an intersection of potential curves and the other, path no. 1, not) then we obtain the following expressions [57] by substituting equations (4.30), (4.31), (4.21) and (4.19b) into equation (4.27)

$$\sigma_1(E_c) = \frac{g\pi}{\mu E_c} \int_0^{J_{max}} \frac{\Delta'_1}{\Delta'_1 + \Delta'_2}\, dJ \tag{4.32}$$

$$\sigma_2(E_c) = \frac{\pi}{\mu E_c} \int_0^{J_{max}} \frac{\Delta'_2}{\Delta'_1 + \Delta'_2}\, dJ \tag{4.33}$$

where

$\sigma_1(E_c)$, $\sigma_2(E_c)$ are the reaction cross-sections for paths 1 and 2 respectively,

$\Delta'_1 = \frac{1}{2}[E^+ - J^3/(54C\mu^3)^{1/2}]^2$

and

$\Delta'_2 = 2A_2[E^+ - J^3/(54C\mu^3)^{1/2}]^{3/2}$, A_2 being the Landau-Zener coefficient for path 2.

In deriving (4.32) and (4.33) the value of S_{eff} has been taken to be 2. This is the "loose complex" limit for a triatomic activated complex [60]. Furthermore, the normalized angular momentum distribution has been taken to be [60]

$$\rho(J) = 2J/J_{max}^2 \qquad \text{for } J < J_{max} \tag{4.34a}$$

and

$$\rho(J) = 0 \qquad \text{for } J > J_{max} \tag{4.34b}$$

The value of J_{max} is the value of angular momentum corresponding to the maximum value of V_{eff} (the centrifugal potential). From (4.26) it follows that

$$J_{max} = (54E_c^2C\mu_i^3)^{1/6} \tag{4.35}$$

The total cross-section $\sigma_T(E_c)$ for the reaction (denoted by equation (4.1a) is hence

$$\sigma_T(E_c) = \sigma_1(E_c) + \sigma_2(E_c) \qquad (4.36)$$

4.2.2 Vibrational Energy Content of Products

An estimate of the product vibrational energy is essential for the analysis of any infrared diatomic laser, since such a laser would require a partial vibrational-rotational population inversion. It is therefore necessary to calculate the extent to which the exothermicity of the quenching process is partitioned into product vibration.

In order to estimate the extent of vibrational excitation in the products formed by dissociation of the activated complex, it is necessary to make certain assumptions regarding how the energy of the complex evolves into translational and internal motion of the products.

Tully [60] makes the assumption that the total rotational energy of products equals rotational energy at critical configuration, vibrational energy of products equals vibrational energy at critical configuration and translational energy of products equals the sum of the translational energy at critical configuration plus the effective potential energy $B_i^+(J)$.

This leads [60] to the following expression for the partial cross-section for production of vibrational energy in the diatomic molecule (AB in (4.1a) above)

$$\sigma_v(E^+;E_v) = \sigma_{cc}(E_c) \int_0^{J_{max}} \frac{2J}{J_{max}^2} \frac{1}{\Delta'_1 + \Delta'_2} \int^{E^+-B_i^+(J)-E_v^+} [1-\exp(-A_2/E_t^+)^{1/2})]$$

$$dE_t^+ dJ \qquad (4.37)$$

where

E_v is the vibrational energy of the diatomic.

(The other symbols have been defined previously).

Application to the Na^*-H_2 quenching process

A computer program utilizing the Romberg technique of integration [70] has been developed to evaluate integrals of the types shown in equations (4.32), (4.33) and (4.37) above. (Appendix VII gives details of the program). This routine was tested by duplicating the results of Tully [60] for quenching of electronically excited Oxygen atoms by Nitrogen molecules

$$O(^1D) + N_2 \rightarrow O(^3P) + N_2(v) \qquad (4.38)$$

(The theoretical results obtained by using Tully's analysis predict an efficiency of about 30% for this E-V transfer process, in very good agreement with the experimental results of Slanger and Black [71] who report that an average of 33% of the 1.98 ev exothermicity goes into N_2 vibrations).

The reaction denoted by equation (4.39) below which results in vibrational excitation of Hydrogen molecules has been known for quite some time [52,39]

$$Na(3^2P) + H_{2_v} \rightarrow Na(3^2S) + H_{2_{v'}} \quad v' > v \qquad (4.39)$$

where

v and v' are the initial and final vibrational quantum numbers.

Quenching of the excited Sodium atoms occurs via the formation of a loosely bonded ionic complex, $Na^+H_2^-$ the only restriction being that the Hydrogen bond be extended initially [52]. (Hence, in (4.39), $v \neq 0$). The RRKM theory of unimolecular decomposition described above can, therefore be applied to this process.

The reaction indicated by equation (4.39) is not spin-forbidden, in contrast to the quenching of excited Oxygen atoms by Nitrogen molecules (4.38). Therefore, Tully's extension of the RRKM theory would be expected to yield only a rough estimate for the vibrational energy content of H_2. The use of the theory can, however, be justified on the grounds that Tully's formulation is fairly insensitive to the Landau-Zener coupling coefficient A_2 (this being the reason why the approximate Landau-Zener expression could be used in the first place) and because the most important criteria are the formation of an activated complex and an intersection of potential energy curves. Both these criteria are satisfied by reaction (4.39).

The relevant potential energy curves are shown in Figure 4.7.

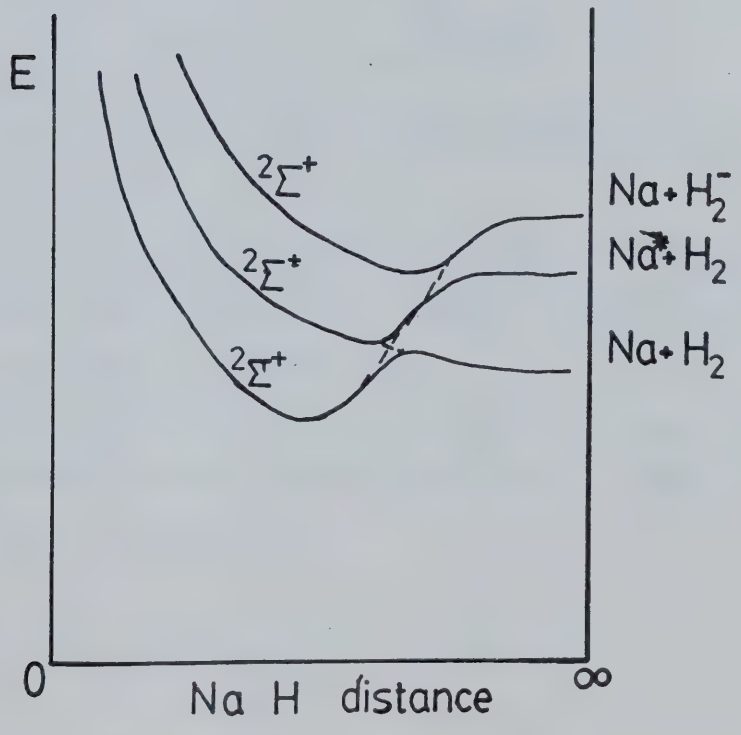

Figure 4.7 Potential Energy Curves for the Na-H_2 System (assuming linear Configuration [52]

Magee and Ri [72] have shown that the activated complex in process (4.39) is actually triangular in configuration (see Figure 4.8)

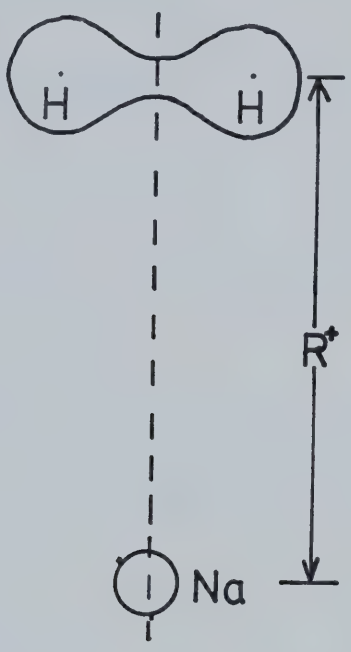

Figure 4.8 Configuration of the $Na^{+}H_2^{-}$ Complex [72]

The potential energy curves in Figure 4.7 are, strictly speaking, valid for a linear configuration. However, the error induced as a result of this assumption is negligible [52].

To be able to evaluate the total quenching cross-section (equation (4.27)) and the partial vibrational cross-section (equation (4.37)), the following data were used:

μ = 1.84 a.m.u.

C = 51.2 ev$(\mathring{A})^6$

E^{+} = 2.09 ev/molecule

V_2 = - 1.6 ev

R_2^+ = 2.7 Å

A_2 = 0.017 $(ev)^{1/2}$/molecule

(See Appendix VIII for a note on units).

$\mu = \frac{M_{H_2} M_{Na}}{M_{H_2} + M_{Na}}$ is the reduced mass of the activated complex,

where M_{H_2}, M_{Na} denote the masses of H_2 and Na, respectively. Using M_{H_2} = 2 a.m.u M_{Na} = 23 a.m.u. yields μ = 1.84 a.m.u.

C is the van der Waals' coefficient for the Na-H_e system. This can be calculated from the combination rule for van der Waals' force constants [73]. This rule gives for a system a-b of particles the following value:

$$C_{ab} \simeq \frac{2\, C_{aa}\, C_{bb}}{(\alpha_b/\alpha_a)C_{aa} + (\alpha_a/\alpha_b)C_{bb}} \qquad (4.40)$$

where

the C's are the induced-dipole-induced-dipole van der Waals coefficients for pairwise interactions of atoms a and b,

and

the α's are the static dipole polarizabilities.

Using the values given by Kramer and Herschbach [73] equation (4.40) yields

$$C_{Na-H_2} \simeq \frac{2 \times 1580 \times 13.0}{\frac{5.33}{165} \times 1580 + \frac{165}{5.33} \times 13.0} \times 0.96 \times 10^{-6} \text{ erg cm}^6$$

$C_{Na-H_2} \simeq 51.2 \text{ ev}(\mathring{A})^6$

E^+ is the exothermicity of the reaction

$E^+ = 2.09$ ev [39]

The values of R^+ and V_2^+ are obtained from Figure 4.7 which is taken from reference [52].

The value of the Landau-Zener coupling coefficient, A_2, is uncertain for the quenching of Sodium by Hydrogen. However, as pointed out previously, the formulation given above, is not very sensitive to variations in A_2. The value of A_2 used here is taken from Yamanouchi and Horie [74] and is the value for quenching of excited Oxygen by Nitrogen molecules.

The graph in Figure 4.9 summarizes the results of the computations done. It is seen that at the lower collisional energies, E_c, the percentage of exothermicity which goes into vibration is larger than that at higher temperatures. The total quenching cross-sections show a similar trend. This behaviour is to be expected because at very high temperatures the duration of the collision becomes so short that the particles do not interact by any significant amount. Note that the calculated values of vibrational cross-section [$\simeq 10(\mathring{A})^2$] for the excitation of the second vibrational level are in fair agreement with the experimental value [$\simeq 15(\mathring{A})^2$] quoted by Pringsheim [79]. [The latter value is for excitation of the fourth vibrational level. However, since the RRKM theory for E-V transfer predicts that vibrational cross-sections are not heavily dependent on the resonant defect - and this has been verified experimentally [39] - we would expect the experimental cross-section for excitation of the second level to be about $15(\mathring{A})^2$ too].

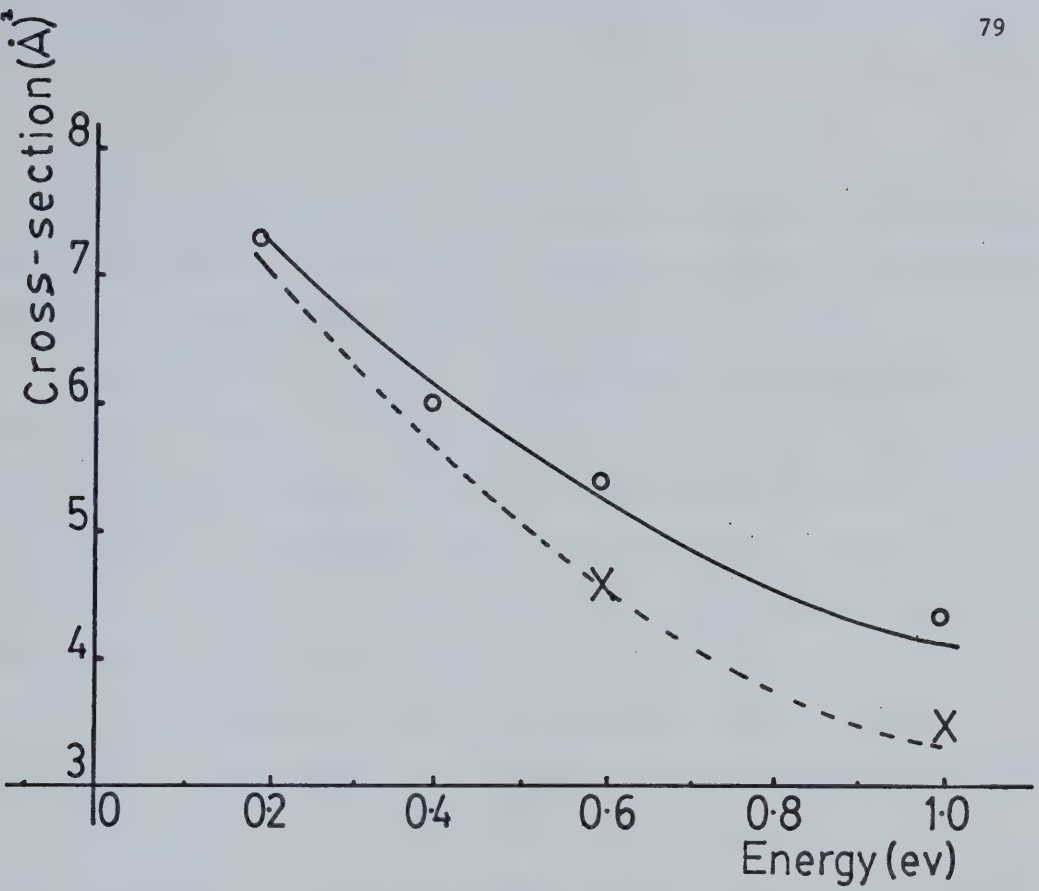

Figure 4.9 Computed total and partial-vibrational cross-sections for quenching of Na^* by H_2.

4.3 The Born-Oppenheimer Approximation and Electronic-to-Vibrational Energy Transfer

The Born-Oppenheimer Approximation allows the total wavefunction of a molecular system to be separated into the product of nuclear and electronic wavefunctions. The total energy of the molecule is also separable, by this approximation, into the sum of nuclear and electronic energies.

The importance of this approximation to the E-V transfer problem lies in the fact that if, in an interacting system of particles, the nuclear and electronic motions are *not* separable then it might be expected that the E-V and V-E processes would occur with high efficiency. The

breakdown of the approximation and the consequent mixing of electronic and nuclear wavefunctions allows efficient conversion of energy from electronic to nuclear (vibrational and rotational) forms and vice versa.

This statement is verified by the fact that interconversion of electronic and vibrational energies occurs with high efficiencies in systems where the potential energy curves of the final and initial states cross with formation of a collision complex at the intersection. This is exactly the condition where the Born-Oppenheimer Approximation breaks down, as will be shown below.

This Approximation was first derived in 1927 [75]. The original derivation is fairly complex [76] and there has been little work done since then in this field. However, the validity of the approximation has been proved theoretically, for a simple system recently [77]. The Approximation has been verified, at least indirectly, by experimental evidence. Hence, for example, since the Franck-Condon Principle [76] is based on this approximation and since many molecular phenomena have been explained by the former, it may be said that the Born-Oppenheimer Approximation has been proved experimentally. The E-V transfer process provides indirect experimental evidence for the validity of the approximation, also as explained above.

It is, perhaps, interesting to note that the Franck-Condon Principle rests on the validity of the Born-Oppenheimer Approximation. Efficient E-V transfer, on the other hand, relies on the breakdown of the approximation.

Derivation of the Approximation [78]

Classically, the picture that forms the conceptual basis of the

Born-Oppenheimer Approximation is one in which electrons are visualized as light and extremely swift particles "whizzing furiously" around heavy, and sluggish nuclei. It might be expected that the electrons complete traversing one or more orbits before the nuclei move even a very small distance. This model is based on the fact that nuclei are immensely more massive than electrons. The same Coulomb force would consequently give an electron a much higher acceleration (and hence a much higher terminal speed) than it would a nucleus.

To derive the approximation quantitatively, however, we have to resort to quantum mechanics.

The starting point is the Schroedinger time independent equation

$$H(\bar{r}_i,\bar{R}_\alpha)\ \psi_E(\bar{r}_i,\bar{R}_\alpha) = E\psi_E(\bar{r}_i,\bar{R}_\alpha) \qquad (4.41)$$

where

$\bar{r}_i$, $\bar{R}_\alpha$ denote the radius vectors to the electron i, and the nucleus, α,

E denotes the energy of the stationary state described by equation (4.41),

H is the Hamiltonian Operator for the system.

$$H(\bar{r}_i,\bar{R}_\alpha) = -\frac{h^2}{2M_e}\sum_{i=1}^{N_e}\nabla_i^2 - \sum_{\alpha}^{N_\alpha}\frac{h^2}{2M_\alpha}\nabla_\alpha^2 + V(\bar{r}_i,\bar{R}_\alpha) \qquad (4.42)$$

The first two terms in equation (4.42) are the Kinetic Energy operators for the N_e electrons and the N_α nuclei in the molecule. $V(\bar{r}_i,\bar{R}_\alpha)$ represents the total potential energy of the molecular system under consideration. The notation used is illustrated in Figure 4.10.

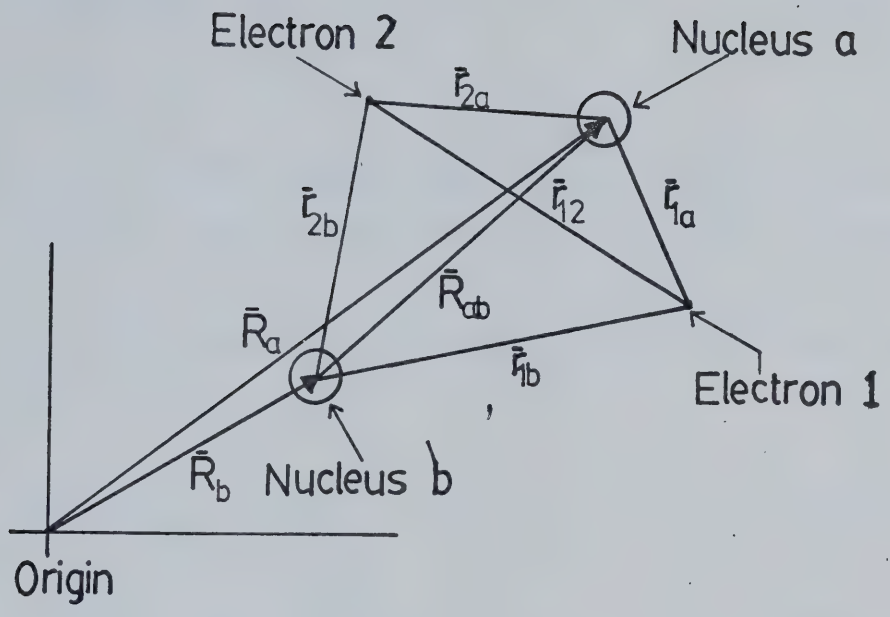

Figure 4.10 A symbolic sketch of a molecule showing electronic and nuclear coordinates

The potential energy term, $V(\bar{r}_i, \bar{R}_\alpha)$, used in the derivation below will consist only of the Coulomb interaction terms V_{ee}, V_{en} and V_{nn}, to be defined later. Strictly speaking, other terms like the one due to Spin-Orbit interaction, ought to be included if $V(\bar{r}_i, \bar{R}_\alpha)$ is to represent the total potential energy function for the system. However, such terms are small (Spin-Orbit coupling, for example, is a relativistic effect) and could, if necessary, be treated by Perturbation Theory. It should be noted, however, that the Born-Oppenheimer theory is valid regardless of whether these terms are neglected or not [78].

We write $V(\bar{r}_i, \bar{R}_\alpha)$ as

$$V(\bar{r}_i,\bar{R}_\alpha) = V_{ee} + V_{en} + V_{nn} \tag{4.43}$$

where

V_{ee} is the Coulomb potential term for electron-electron interactions,

V_{en} is the Coulomb potential term for electron-nucleus interactions

and

V_{nn} is the Coulomb potential term for nucleus-nucleus interactions.

Therefore,

$$V_{ee}(\bar{r}_i) = \sum_{(ij)} \frac{e^2}{|\bar{r}_i - \bar{r}_j|} \tag{4.44a}$$

$$V_{en}(\bar{r}_i,\bar{R}_\alpha) = \sum_{(i\alpha)} - \frac{Z_\alpha e^2}{|\bar{r}_i - \bar{R}_\alpha|} \tag{4.44b}$$

$$V_{nn}(\bar{R}_\alpha) = \sum_{(\alpha\beta)} \frac{Z_\alpha Z_\beta e^2}{|\bar{R}_\alpha - \bar{R}_\beta|} \tag{4.44c}$$

where

the notations (ij), (iα) and (αβ) on the summations imply that each pair of particles has to be included just once,

Z_α, Z_β represent the charges on the nuclei α and β respectively,

and

e is the electronic charge.

If the Kinetic Energy Operators in equation (4.42) are denoted by $T_e(\bar{r}_i)$ and $T_n(\bar{R}_\alpha)$, i.e.

$$T_e(\bar{r}_i) = - \frac{h^2}{2M_e} \sum_{i=1}^{N_e} \nabla_i^2 \tag{4.45a}$$

and

$$T_n(\bar{R}_\alpha) = -\frac{h^2}{2} \sum \frac{1}{M_\alpha} \nabla_\alpha^2 , \qquad (4.45b)$$

then the total molecular Hamiltonian becomes

$$H(\bar{r}_i, \bar{R}_\alpha) = T_e(\bar{r}_i) + T_n(\bar{R}_\alpha) + V_{ee}(\bar{r}_i) + V_{en}(\bar{r}_i, \bar{R}_\alpha) + V_{nn}(\bar{R}_\alpha) \qquad (4.46)$$

Dropping the coordinate dependence of each term, for convenience, equation (4.41) becomes, after substitution of (4.46),

$$(T_e + T_n + V_{ee} + V_{en} + V_{nn})\, \psi_E = E\, \psi_E \qquad (4.47)$$

Defining

$$H^e = T_e + V_{ee} \qquad (4.48a)$$

$$H^n = T_n + V_{nn} \qquad (4.48b)$$

$$H^{en} = V_{en} \qquad (4.48c)$$

equation (4.47) can be written as

$$(H^e + H^n + H^{en})\, \psi_E = E\, \psi_E \qquad (4.49)$$

The Born-Oppenheimer Approximation can now be stated mathematically.

The total wave function ψ_E (equation (4.41)) of a molecular system can be approximated, under certain restrictions, to the product

$$\psi_E(\bar{r}_i,\bar{R}_\alpha) = \psi^e(\bar{r}_i;\bar{R}_\alpha) \cdot \psi^n(\bar{R}_\alpha) \tag{4.50}$$

where

$\psi^e(\bar{r}_i;\bar{R}_\alpha)$ is the solution to the equation:

$$(T_e + V_{ee} + V_{en})\ \psi^e = E^e\psi^e \tag{4.51}$$

and

$\psi^n(\bar{R}_\alpha)$ is the solution to the equation:

$$(T_n + V_{nn} + E^e)\ \psi^n = E^n\psi^n \tag{4.52}$$

Furthermore, the total energy of the molecular system can, under the same restrictions, be approximated as

$$E \simeq E^n \tag{4.53}$$

The energy operators in equation (4.51) and (4.52) are defined as the *electronic* and *nuclear* Hamiltonians, respectively.

It should be noted that equations (4.52) and (4.53) give validity to the potential energy diagrams for any molecule. Equation (4.52) states that the nuclear motion in a molecule takes place in an effective potential energy function $(V_{nn} + E^e)$. This is the potential function usually drawn

in energy level diagrams. The effect of different electronic states is incorporated in this effective potential function by the term E^e which is the solution to the electronic equation (4.51). Furthermore, equation (4.53) states that the total energy of the molecular system is the eigenvalue of equation (4.52).

Should the Born-Oppenheimer Approximation break down, then equations (4.50), (4.51), (4.52) and (4.53) no longer hold. In that case, the potential energy diagram concept, strictly speaking, has no validity either.

The conditions under which the Born-Oppenheimer Approximation holds will now be derived. It will be assumed first that the approximation holds (and that, therefore, the nuclear and electronic motions can be separated). An analysis will be made to then derive the conditions which have to be satisfied in order that the assumption of separable wavefunctions be valid.

Using equations (4.48) we rewrite (4.51) and (4.52) as,

$$(H^e + H^{en})\ \psi^e(\bar{r}_i,\bar{R}_\alpha) = E^e(\bar{R}_\alpha)\ \psi^e(\bar{r}_i;\bar{R}_\alpha) \qquad 4.54)$$

and

$$(H^n + E^e)\ \psi^n(\bar{R}_\alpha) = E^n\psi^n(\bar{R}_\alpha) \qquad (4.55)$$

respectively.

We expand ψ_E [in (4.41)] as a series:

$$\psi_E = \psi^e\psi^n + \psi^{(1)} + \psi^{(2)} + \ldots \qquad (4.56)$$

Similarly E [in equation 4.41] is written as:

$$E = E^n + E^{(1)} + E^{(2)} + \ldots \tag{4.57}$$

We have then to find the conditions under which the second and following terms in (4.56) and (4.57) are negligible compared to the first terms in these two equations.

Substituting (4.56) and (4.57) into the Schroedinger equation (4.41) yields

$$H(\psi^e\psi^n + \psi^{(1)} + \psi^{(2)} + \ldots) = (E^n + E^{(1)} + E^{(2)} + \ldots)(\psi^e\psi^n + \psi^{(1)} + \psi^{(2)} + \ldots) \tag{4.58}$$

Therefore,

$$H\psi^e\psi^n + H\psi^{(1)} + \ldots = E^n\psi^e\psi^n + E^{(1)}\psi^{(e)}\psi^{(n)} + E^n\psi^{(1)} + \ldots \tag{4.59}$$

Using $H = H^e + H^n + H^{en}$ we find

$$H\psi^e\psi^n = E^n\psi^e\psi^n + [T_n,\psi^e]\psi^n \tag{4.60}$$

where

$[T_n,\psi^e]$ represents the commutator operator defined by

$$[T_n,\psi^e] = T_n\psi^e - \psi^e T_n.$$

Note that equations (4.54) and (4.55) have been used to derive equation (4.60).

Using (4.59) in (4.60) and ignoring terms of second and higher order yields,

$$[T_n,\psi^e]\psi^n + H\psi^{(1)} = E^n\psi^{(1)} + E^{(1)}\psi^e\psi^n \tag{4.61}$$

$\psi^{(1)} = \psi^{(1)}(\bar{r}_i,R_\alpha)$ can be written [78] as the sum

$$\psi^{(1)}(\bar{r}_i,\bar{R}_\alpha) = \psi^{(1)}_{\varepsilon\nu}(\bar{r}_i,\bar{R}_\alpha) = \sum_{\varepsilon',\nu'} a^{(1)}_{\varepsilon',\nu'}\,\psi^e_{\varepsilon'}(\bar{R}_i;\bar{R}_\alpha)\cdot$$

$$\psi^n_{\varepsilon',\nu'}(\bar{R}_\alpha) \tag{4.62}$$

where the subscripts $\varepsilon,\nu,\varepsilon'$ and ν' are quantum numbers introduced to distinguish wavefunctions corresponding to different states.

Using this expansion in equation (4.60) we obtain

$$H\psi^{(1)}_{\varepsilon\nu} = \sum_{\varepsilon',\nu'} a^{(1)}_{\varepsilon',\nu'}\,E^n_{\varepsilon',\nu'}\psi^e_{\varepsilon'}\psi^n_{\varepsilon',\nu'} + \sum_{\varepsilon',\nu'} a^{(1)}_{\varepsilon',\nu'}\,[T_n,\psi^e_{\varepsilon'}]\,\psi^n_{\varepsilon',\nu'} \tag{4.63}$$

Ignoring the second term in (4.63) (since it is of second order) and substituting into (4.61) yields

$$[T_n,\psi^e_\varepsilon]\,\psi^n_{\varepsilon\nu} + \sum_{\varepsilon',\nu'} a^{(1)}_{\varepsilon',\nu'}\,E^n_{\varepsilon',\nu'}\,\psi^e_{\varepsilon'}\psi^n_{\varepsilon',\nu'} \tag{4.64}$$

$$= E^n_{\varepsilon\nu}\sum_{\varepsilon',\nu'} a^{(1)}_{\varepsilon',\nu'}\psi^e_{\varepsilon'}\psi^n_{\varepsilon',\nu'} + E^{(1)}_{\varepsilon\nu}\psi^e_\varepsilon\,\psi^n_{\varepsilon\nu}$$

Multiplying both sides of this equation by $\psi^{e*}_{\varepsilon''}$, $\psi^{n*}_{\varepsilon''\nu''}$ (where the asterisks denote complex conjugation) and integrating over all electronic and nuclear coordinates (τ_e and τ_n respectively) results in the following equation [78]:

$$\int \psi^{e*}_{\varepsilon''}\, \psi^{n*}_{\varepsilon''\nu''}[T_n,\psi^e_\varepsilon]\psi^n_{\varepsilon\nu}d\tau_e d\tau_n + a^{(1)}_{\varepsilon''\nu''}\, E^n_{\varepsilon'\nu''}$$

$$= E^n_{\varepsilon\nu}\, a^{(1)}_{\varepsilon''\nu''} + E^{(1)}_{\varepsilon\nu}\, \delta_{\varepsilon\varepsilon''}\, \delta_{\nu\nu''} \qquad (4.65)$$

where

$\delta_{\varepsilon\varepsilon''}$, $\delta_{\nu\nu''}$ are delta-Dirac functions.

Finally, for the case when $\varepsilon \neq \varepsilon''$ and $\nu \neq \nu''$ equation (4.65) yields

$$a^{(1)}_{\varepsilon''\nu''} = \frac{\int \psi^{e*}_{\varepsilon''}\psi^{n*}_{\varepsilon''\nu''}[T_n,\psi^e_\varepsilon]\psi^n_{\varepsilon\nu}d\tau_e d\tau_n}{E^n_{\varepsilon\nu} - E^n_{\varepsilon''\nu''}} \qquad (4.66)$$

This is the result being sought since it provides a condition for the validity of the Born-Oppenheimer Approximation. If all the coefficients $a^{(1)}_{\varepsilon''\nu''}$ were small compared to unity ($a^{(1)}_{\varepsilon''\nu''} << 1$) then the first order correction to the wavefunction, $\psi^{(1)}_{\varepsilon\nu}$ in equation (4.62) would be small compared to the zeroth order term $\psi^e\psi^n$ in equation (4.56). In that case

$$\psi_E \simeq \psi^e\psi^n \qquad (4.67)$$

which is the Born-Oppenheimer Approximation.

In general, the commutator in equation (4.66) is not zero. It is seen therefore that $a^{(1)}_{\varepsilon''\nu''}$ would be large near a region where electronic

degeneracy exists. (i.e. where $E^n_{\varepsilon\nu} = E^n_{\varepsilon'',\nu''}$). In other words, it can be stated that in general near a region of potential energy curve crossing the Born-Oppenheimer Approximation breaks down.

Now, the experimentally verified fact that efficient E-V transfer occurs if the potential energy curves of the final and initial states of the system intersect, can be understood. It has been shown that near the region of crossing the Born-Oppenheimer Approximation fails resulting in a mixing of electronic and vibrational wavefunctions. Under these circumstances, it is logical to assume that efficient E-V transfer would occur. Furthermore, viewed from this light, the fact (again experimentally verified) that a loosely bonded collision complex around the region of curve crossing greatly enhances the efficiency of the process, is understandable also. A collision complex having a lifetime of a few vibrational periods would allow enough time for the mixing of wavefunctions, predicted by the theory, thus increasing the efficiency of the E-V process.

CHAPTER V

CONCLUSION AND OUTLOOK

The problem of obtaining a population inversion in the vibrational-rotational energy levels of the Hydrogen molecule is perhaps best suited to optical pumping.

The small dissociation energy of the molecule and the strong electronegative character of the Hydrogen atom make pumping by the electric-discharge or e-beam technique difficult. This is all the more so at high pressures. The development of high energy-high power H_2 infrared lasers must await the overcoming of these difficulties.

On the other hand, it seems feasible that optically pumped H_2 lasers could be developed using technology available at present. Such lasers would, of necessity, be low energy output devices. The advantages of a high pressure tunable IR laser in the 2μm region of the spectrum, however, make the effort worthwhile.

Optical excitation of a metastable electronic state (of an atom or a molecule) which then transfers its energy to vibrations of H_2 seems to be the most promising technique, since the efficiency of an E-V transfer process can be quite high under suitable circumstances, as illustrated in Chapter IV. In particular, if the collision complex model holds for a given system then the efficiency of the transfer process would, as a rule, be high. This is because, as Tully's formulation shows, the model is not very sensitive to some of the parameters (e.g. the Landau-Zener coefficient).

There is scope for extension of the theory to incorporate the effect of pressure explicitly. Since the RRKM expression reduces to the Activated Complex formulation in the high pressure limit, the basic mechanism of E-V

transfer does not change. However, it would be very useful to have a quantitative formulation for the effect of pressure on the vibrational partial cross-sections. The effect of deactivating collisions would be important at high pressures and this ought to be considered too.

But, perhaps, the greatest scope is presented when the whole E-V transfer process is viewed in terms of the breakdown of the Born-Oppenheimer Approximations and consequent mixing of electronic and nuclear motions. It is known that this occurs near a region of electronic degeneracy. It would be fruitful to formulate general criteria for the breakdown of this approximation. The criteria would probably be based on symmetry considerations It would not be necessary to solve completely for either the wavefunctions or the Hamiltonian for the interacting system of particles. On this basis, and making the further restriction that the system form a loosely bonded complex, various possible atoms and molecules might be investigated as prospective candidates for pumping various molecules including H_2. (E-V transfer between molecules has been demonstrated for the first time, by Slanger and Black, recently [80]).

To illustrate the above points, consider a two level system.

It can be shown [81] that the energies of such a system are given by

$$E_{1,2} = \frac{1}{2}(H_{11} + H_{22}) \pm \frac{1}{2}\{(H_{11} - H_{22})^2 + 4|H_{12}|^2\}^{1/2} \qquad (5.1)$$

where

$H_{ij} = \langle\psi_i|H|\psi_j\rangle = \int_\tau \psi_i^* H\psi_j \, d\tau$, and

τ is the volume over which the integral is evaluated.

In this case a necessary, but insufficient condition for degeneracy is

$$\langle \psi_1 | H | \psi_2 \rangle = 0 \qquad (5.2)$$

If the symmetries of ψ_1, ψ_2, and the Hamiltonian are known then it would be possible to see whether or not, for a given system of interacting particles, equation (5.2) holds. It is not necessary to have complete information on these quantities, only the symmetry properties have to be known.

A development of these ideas, bearing in mind that there exists a close relationship between the breakdown of the Born-Oppenheimer criterion and efficient E-V transfer should offer a powerful basis for selecting any atom or molecule to pump another by this process.

APPENDIX I

SOME TUNABLE LASERS IN THE INFRARED

Some of the tunable semiconductor lasers in the IR region of the spectrum which are presently available are shown in Figure A1 below [3].

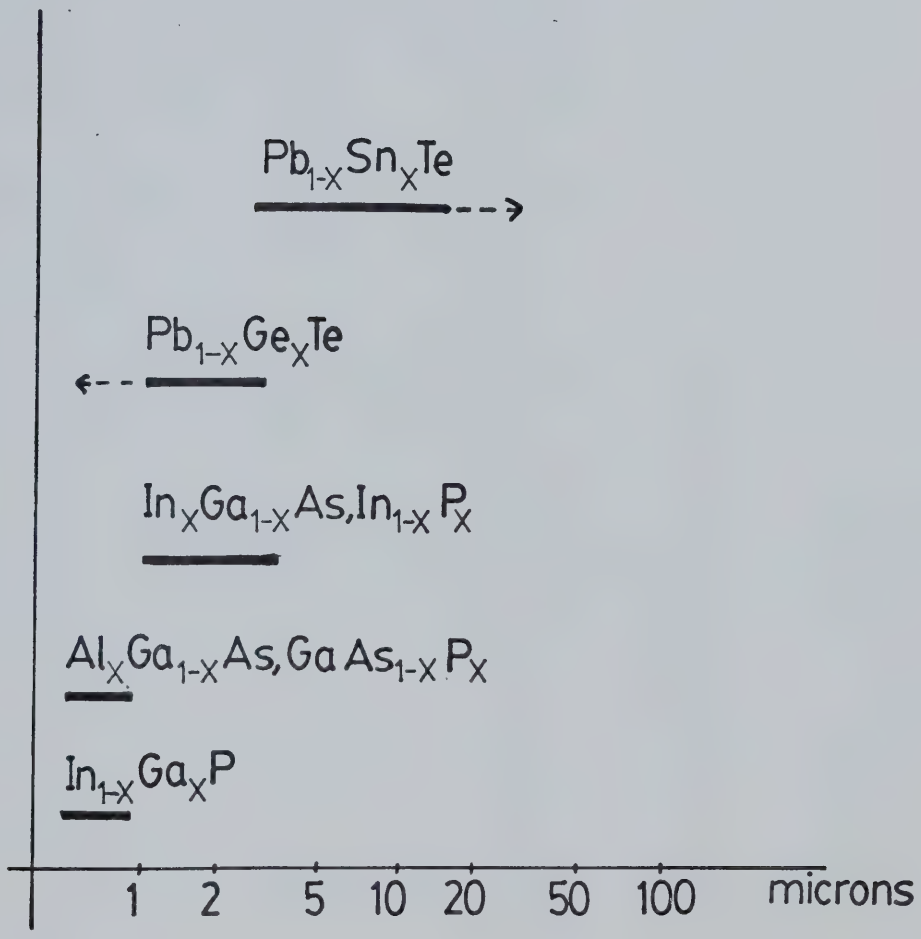

Figure A1 Wavelength Ranges Covered by Various Semiconductor Lasers [3]

High pressure tunable CO_2 gas lasers have also been reported by various workers [10, 11, 12]. These are lasers operating in the 10μm region.

APPENDIX II

VIBRATIONAL BAND FOR H_2

The table below lists the frequencies and wavelengths of transitions between adjacent vibrational levels of H_2 for its ground electronic ($^1\Sigma_g^+$) state.

The following approximate equation [18] for the vibrational term value has been used:

$$G_o(v) \simeq \omega_o v - \omega_o x_o v^2 \qquad \text{(A2.1)}$$

where

v is the vibrational quantum number, $\omega_o \simeq \omega_e - \omega_e x_e$

and

$\omega_o x_o \simeq \omega_e x_e$

the values for ω_e and $\omega_e x_e$ being taken as 4935 cm^{-1} and 117 cm^{-1} respectively. Hence, the energy for the transition between levels $v'' = v$ and $v' = v + 1$ is

$$G_o(v') - G_o(v'') = G_o(v+1) - G_o(v) \simeq \omega_o - \omega_o x_o [(v')^2 - (v'')^2] \qquad \text{(A2.2)}$$

Note the anharmonic defect between the lowest two frequencies is $\Delta\nu = 0.7 \times 10^{13}$ Hz

$$h\Delta\nu = \Delta E = 2.9 \times 10^{-2} \text{ ev} \simeq 3 \times 10^{-2} \text{ ev}$$

Table A2: Vibrational Transition Frequencies for H_2

Transition $v' \rightarrow v''$	Frequency x 10^{13}Hz	Wavelength μm
15→14	4.2	7.01
14→13	5.0	6.03
13→12	5.7	5.28
12→11	6.4	4.70
11→10	7.1	4.24
10→ 9	7.8	3.85
9→ 8	8.5	3.53
8→ 7	9.2	3.26
7→ 6	9.9	3.04
6→ 5	10.6	2.83
5→ 4	11.3	2.66
4→ 3	12.0	2.50
3→ 2	12.7	2.36
2→ 1	13.4	2.24
1→ 0	14.1	2.13

This compares well with the value, 5×10^{-2} ev obtained from equation (1.9).

APPENDIX III

RADIATION TRANSITION PROBABILITIES [18]

In the presence of electromagnetic radiation the total Hamiltonian for an atom or molecule must include the energy term due to interaction between the radiation and system of particles.

For instance, if $\bar{M}$ is the dipole moment of the atom or molecule defined by

$$\bar{M} = \bar{a}_x M_x + \bar{a}_y M_y + \bar{a}_z M_z$$

where

$\bar{a}_x$, $\bar{a}_y$ and $\bar{a}_z$ are the unit vectors in the x,y, and z directions respectively,then the dipole moment interaction energy term is $\bar{M} \cdot \bar{E}$ ($\bar{E}$ being the electric field intensity vector of the radiation).

The *matrix elements of the electric dipole moment* for energy levels m and n are defined as

$$\bar{R}_x^{mn} = \int \psi_n^* M_x \psi_m d\tau \qquad \text{(A3.2a)}$$

$$\bar{R}_y^{mn} = \int \psi_n^* M_y \psi_m d\tau \qquad \text{(A3.2b)}$$

and

$$\bar{R}_z^{mn} = \int \psi_n^* M_z \psi_m d\tau \qquad \text{(A3.2c)}$$

where

ψ_m, ψ_n are the eigenfunctions of the energy levels under consideration

and

the integration is carried over all space.

The matrix element

$$\bar{R}^{mn} = \bar{a}_x R_x^{mn} + \bar{a}_y R_y^{mn} + \bar{a}_z R_z^{mn}$$

defines the *dipole transition probability* for a m→n or n→m transition.

It can be shown that if $\bar{R}^{mn}$ is zero then the transition is *forbidden* as a dipole transition, otherwise not. *Magnetic dipole*, *quadrupole* and *induced dipole* transition probabilities are defined in a similar manner. In these cases, the corresponding quantity - magnetic dipole moment, quadrupole moment or induced dipole moment (due to either the efi or cid effects or a combination of the two) is substituted in equations (A3.2) instead of M_x, M_y and M_z.

APPENDIX IV

MARX GENERATOR CIRCUIT

A ten stage Marx generator, shown in Figure A4.1, was designed for the electric discharge experiments described in Chapter II.

To prevent arcing, the whole circuit was put in a tank of transformer oil.

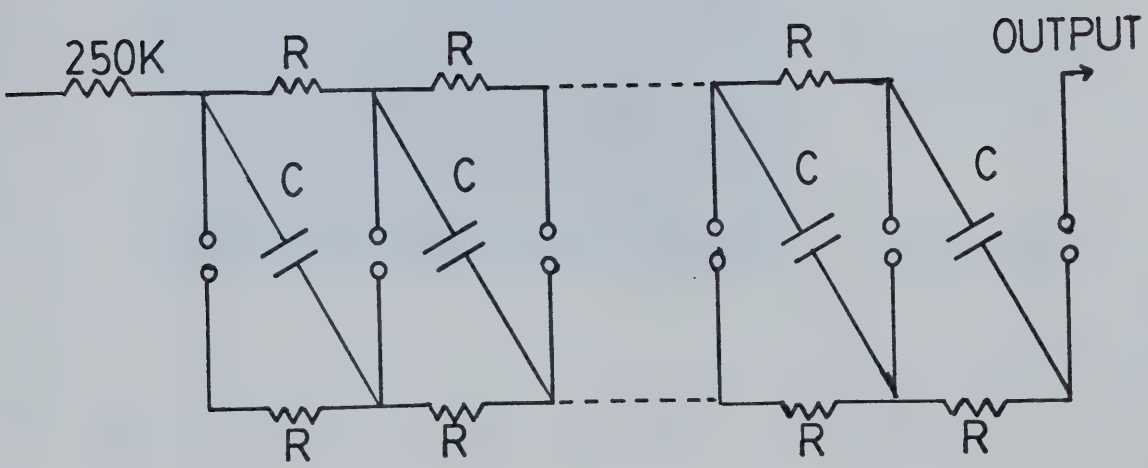

Figure A4.1 Ten Stage Marx Generator

The output voltage from the Marx as measured across a 145 diluted Copper Sulphate resistor is shown in Figure A4.2.

Control over the output voltage pulse magnitude was obtained by varying the pressure of N_2 in the spark gaps. For this best results (an output range of between 100 and 170 KV) were obtained when the sides of spark gaps containing the triggering pins were grounded.

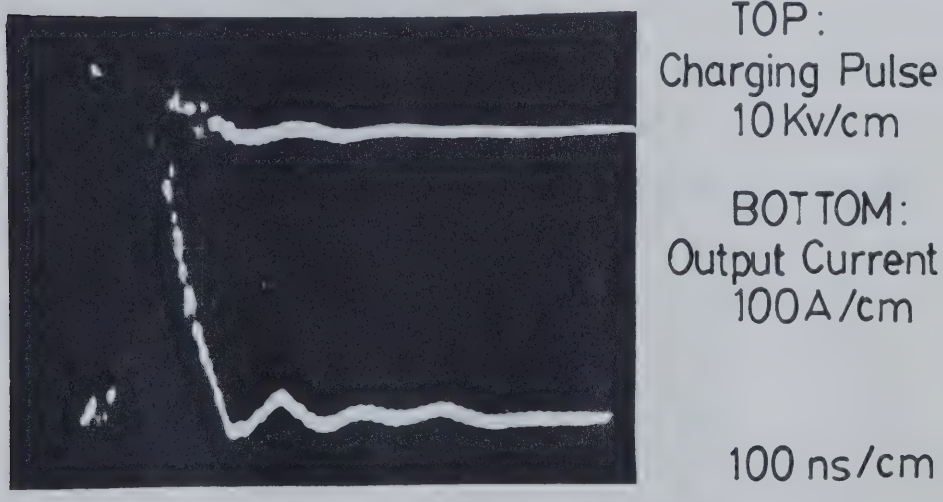

Figure A4.2 Charging and Output Voltage Pulses from the Marx

For the discharge experiments described in Chapter II the Marx was fired at a rate of about one pulse per second or slower.

APPENDIX V

CHEMICAL KINETIC NOTATION [57]

The following list defines the more important of the symbols used in Chapter IV. An attempt has been made to correlate the present notation with that of other authors, the latter being given in brackets following our notation. The authors' names are abbreviated as follows:

L → K.J. Laidler *et al* [56]

M → R.A. Marcus *et al* [59]

T → J.C. Tully [60]

Q, Q_v etc	Partition functions [L: Q or q; M:P]
s	Number of vibrational degrees of freedom of a molecule
ν	Vibration frequencies
v	Vibrational quantum numbers
I	Moments of inertia
J	Rotational quantum numbers
E	Energy per molecule [L: ε or E; T:ε]
E_z	Zero-point energy of a molecule [M:E_o;L:ε or E_z]
$P(E_n)$	Number of quantum states of a given system at the quantized energy level E_n
k	Rate constants in general
k_{uni}	First-order rate-constant [L:k']
k_∞	Limiting high-pressure value of k_{uni} [M and L: k^∞]
k_{bim}	Second-order rate-constant [M:k_o]

k_1, k_2 Rate-constants (second-order) for energization and de-energization, respectively [L:k_1, k_{-1}]

$k_a(E^*)$ Rate-constant for conversion of energized molecules to activated complexes in RRKM theory [M:k_a; L:k_2 or k_E; T:$k(\varepsilon, J, E^+)$]

E_o Critical energy for reaction; 'activation energy' [M:E_a; L:ε_a or E_o]

E_{Arr} Arrhenius activation energy

$A_\infty, E_\infty, E_{bim}$ Limiting high-pressure values of A and E_{Arr} and low-pressure value of E_{Arr}

$\rho_{1/2}$ Pressure at which $k_{uni} = \frac{1}{2} k_\infty$

A^*, A^+ Energized molecule and activated complex (L:$A^*, A^{\neq}$]

E^* Total non-fixed energy in the active degrees of freedom of a given energized molecule A^* [L:ε, T:W^*]

E^+ Total non-fixed energy in the active degrees of freedom of a given activated complex A^+ ($E^+ = E_v^+ + E_r^+ + E_t^+$) [L:$\varepsilon^{\neq}$; T:$E^+ + W^+$]

E_v^+, E_r^+, E_t^+ Vibrational, rotational and translational (along the reaction coordinate) components of E^+ [for E_t^+; M:x or E_t^+; L:$\varepsilon_t^{\neq}$; T:E^+]

E_{vr}^+ $E_{vr}^+ = E_v^+ + E_r^+$ (M:E_n^+; L:$\varepsilon_n^{\neq}$)

E_J, E_J^+ Energy of adiabatic rotations in the Jth energy level in A^* and A^+ respectively

$\Delta E_J = E_J^+ - E_J$ [M:E_j, E_j^+; L:ε_j, $\varepsilon_j^{\neq}$]

$N^*(E^*)$ Density of quantum states of A^* (number of energized molecules per unit energy) at energy E^* [T:N^*; M:$N^*(E^*)$ or $\Omega^*(E^*)$]

$N^+(E_{vr}^+, E_t^+)$ Density of quantum states of A^+ having energy E_{vr}^+ in the active degrees of freedom and energy E_t^+ along the reaction coordinate [M:$N_2(E^+-x)$; L:$N_2(\varepsilon^{\neq} - \varepsilon_t^{\neq})$]

$N_{rc}^+(E_t^+)$ Density of quantum states for the translational motion of A^+ in the reaction coordinate with energy E_t^+ [L:$N_1(\varepsilon_t^{\neq})$]

$P(E_{vr}^+)$ Number of vibrational-rotational quantum states of A^+ at the quantized energy level E_{vr}^+ [M:$P(\varepsilon_n^+)$ or $\Omega^+(E_n^+)$; T:N^+]

δ The arbitrary length of region at the top of potential energy barrier which is taken to define the activated complex [M:b]

μ Characteristic mass for motion in the reaction coordinate [M:m;L:$M^{\neq}$]

$k^+(E_t^+)$ Rate constant at which complexes of energy E_t^+ cross the barrier [M:k_3; L;$\dot{\bar{x}}$]

Q_1, Q_1^+ Partition functions for adiabatic rotations in A and A^+ respectively [M:P_1, P_1^+; L:Q_R, $Q_R^{\neq}$]

Q_2, Q_2^+ Partition functions for active degrees of freedom A and A^+ respectively (A^+ has one fewer degree of freedom) [M:P_2, P_2^+; L:Q_a, $Q_a^{\neq}$]

Q, Q^+ Complete vibrational-rotational partition functions for A and A^+ respectively; $Q = Q_1 \cdot Q_2$; $Q^+ = Q_1^+ \cdot Q_2^+$ [M:P, P^+; L:$Q_i, Q_{\neq}$]

APPENDIX VI

A NOTE ON PARTITION FUNCTIONS [57, 58]

Definition

For a molecular system capable of existing in a series of quantized energy levels with energies E_0, E_1, E_2 ...., the total partition function for the molecule is defined as

$$Q = g_o \exp(-E_0/KT) + g_1 \exp(-E_1/KT) + g_2 \exp(-E_2/KT) + \ldots$$

$$= \sum_{i=o}^{\infty} g_i \exp(-E_i/KT) \qquad \text{(A6.1)}$$

where

g_i is the degeneracy (or statistical weight) of the energy level E_i, which may be defined as the number of different independent wave functions of the system with energy E_i (i.e. the number of physically distinct quantum states of that energy).

If the vibrational, rotational and electronic motions in a molecule can be separated then

$$E_T = E_e + E_v + E_r + E_t$$

where

E_T is the total energy of the molecule

E_e, E_v, E_r and E_t are the electronic, vibrational, rotational and translational energies respectively.

Under these conditions it can be shown [58] that the total partition function, Q, may be written as a product of the vibrational, rotational, electronic and translational partition functions.

$$Q = Q_e \cdot Q_v \cdot Q_r \cdot Q_t \qquad \text{(A6.2)}$$

Note that since nuclear and electronic motions are only separable under the conditions of the Born-Oppenheimer approximation, equation (A6.2) holds only if the approximation does.

APPENDIX VII

COMPUTER PROGRAM FOR CALCULATING VIBRATIONAL CROSS-SECTIONS

The Rhomberg method [70] of integration was used to evaluate the total quenching and partial vibrational cross-sections for the de-excitation of Na^* by collisions with H_2.

Figure A7.1 shows the flow chart for the complete program while Figure A7.2 shows the flow chart for the Rhomberg sub-routine.

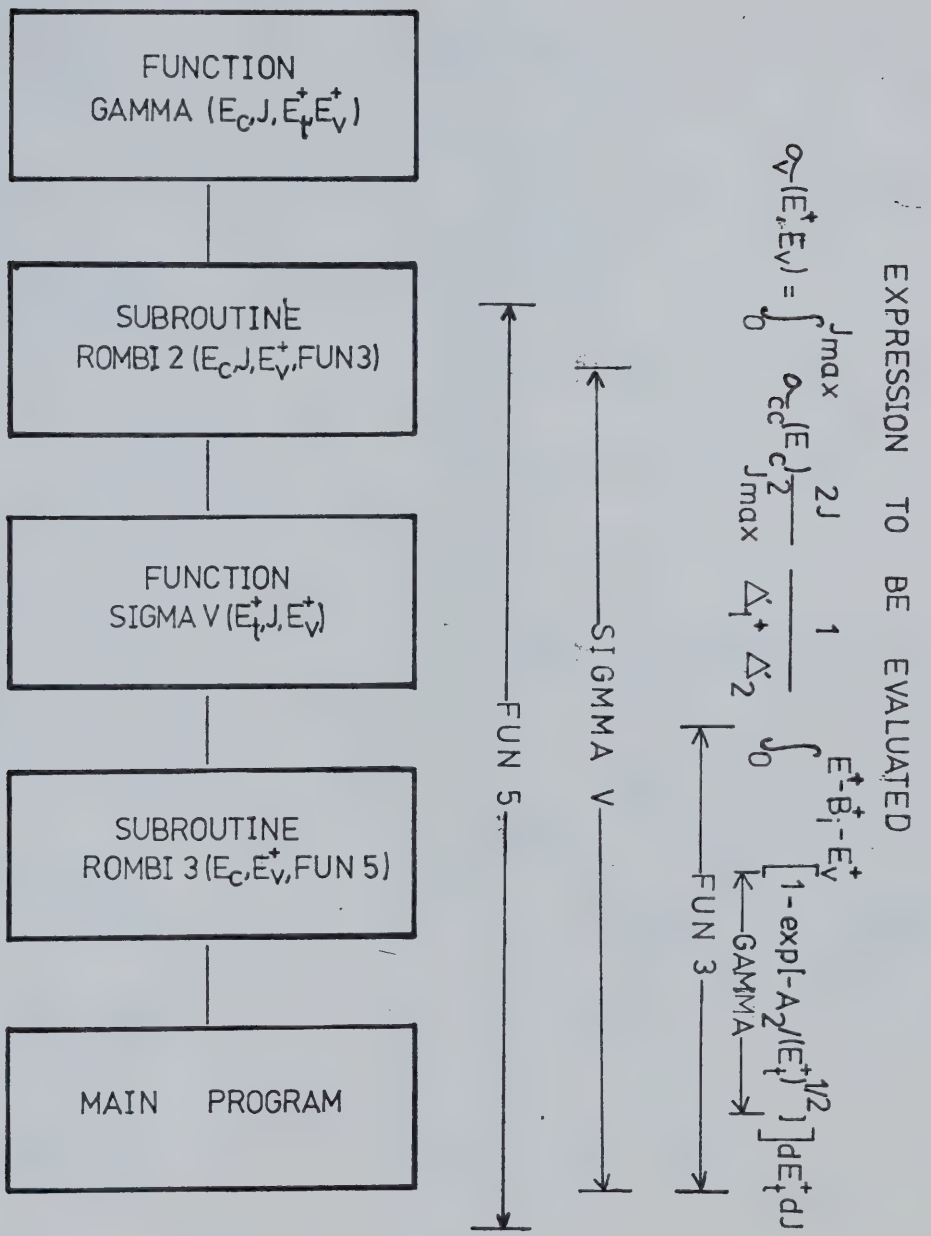

Figure A7.2 Block Diagram of Program Used

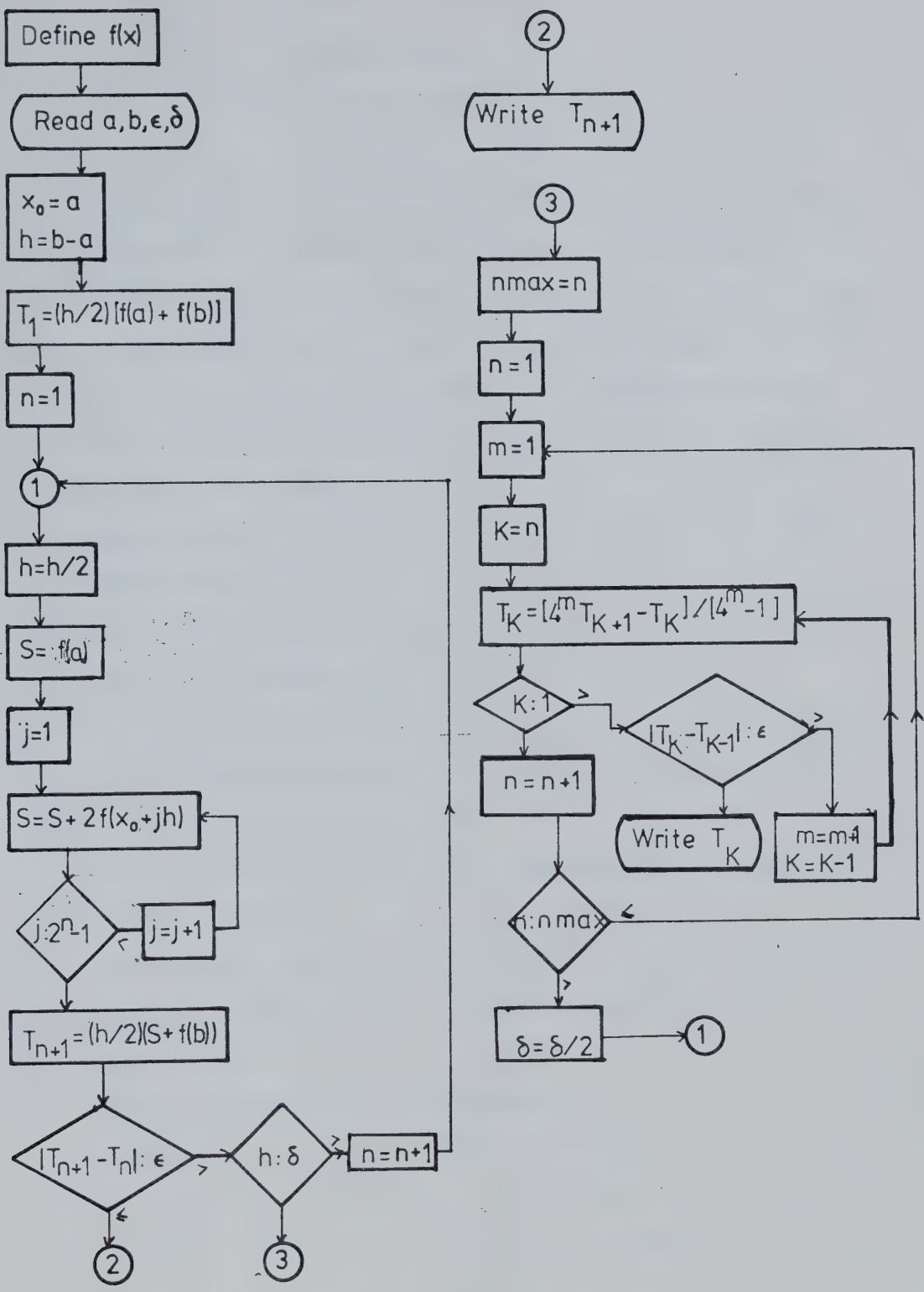

Figure A7.2 The Rhomberg Subroutine [70]

APPENDIX VIII

A NOTE ON ATOMIC UNITS

Since atomic quantities like electronic charge, mass and energies are very small when expressed in ordinary units (c.g.s. or m.k.s) it is necessary, for convenience, to define a system of "Atomic Units". There are many choices available such that the values of fundamental constants, as expressed by these units, are conveniently - handled small numbers. Any system could be used, provided it is based upon the least number of independent quantities [82].

For the computations involved in Chapter IV, the following basic units were defined.

Mass:	(1)atomic mass unit	(a.m.u.)
Energy:	(1)electron volt	(ev)
Length:	(1)$\mathring{A}$ngstrom Unit	($\mathring{A}$)

The units of the other quantities required for computations were defined by using the above three units.

Hence, the units of van der Waals' constant, angular momentum and cross-sections used were,

van der Waal's constant:	$(ev)(\mathring{A})^6$
Angular momentum:	$(ev)^{1/2}(a.m.u.)^{1/2}(\mathring{A})$
Cross-section:	$(\mathring{A})^2$

The following conversion factors apply:

1 a.m.u.	=	1.66×10^{-24} gm
1 ev	=	1.60×10^{-12} erg
$1\ (ev)(\mathring{A})^6$	=	$1.60 \times 10^{-60}(erg)(cm)^6$
$1\ \mathring{A}$	=	10^{-8} cm
$1(ev)^{1/2}(a.m.u.)^{1/2}(\mathring{A})$	=	1.6×10^{-26} erg sec

REFERENCES

[1] N.G. Basov *et al* ., "Possibility of producing tunable infra-red gas lasers," *JETP Lett.*, vol. 14, pp. 375-376. 1971.

[2] H.J. Gerritsen, *Physics of Quantum Electronics*, Ed. Kelley, Lax, Tannenwald. New York: McGraw-Hill, 1965.

[3] I. Melnagilis and A. Mooradin, *Physics of Quantum Electronics*, Ed. S.F. Jacobs, M. Sargent III, J.F. Scott and M.O. Scully. New York: Addison-Wesley, 1975.

[4] R.L. Byer, "A 16μm source for laser isotope enrichment," *IEEE J. Quantum Electron.*, vol. 12, pp. 732-733, 1976.

[5] N.G. Basov *et al.*, "Possibility of generating ultrashort laser pulses on combination vibrational-rotational transitions of molecular Hydrogen," *JETP Lett.*, vol. 16, pp. 211-214, 1972.

[6] P.A. Bazhulin *et al.*, "Stimulated Emission from Molecular Hydrogen and Deuterium in the near Infrared," *Sov. Phys. JETP*, vol. 22, pp. 11-16, 1966.

[7] P.A. Bazhulin *et al.*, "Pulsed laser action in molecular Hydrogen," *Sov. Phys. JETP*, vol. 20, pp. 1068-1069, 1965.

[8] R.V. Ambartsumyan *et al.*, "Isotopic selective chemical reaction of BCl_3 molecules in a strong infrared laser field," *JETP Lett.*, vol. 20, pp. 273-274, 1974.

[9] R.V. Ambartsumyan *et al.*, "Separation of Sulfur isotopes with enrichment coefficient > 10^3 through action of CO_2 laser radiation on SF_6 molecules," *JETP Lett.*, vol. 21, pp. 171-172, 1975.

[10] T.Y. Chang and O.R. Wood, "Optically pumped 33-atm CO_2 laser," *Appl. Phys. Lett.*, vol. 23, pp. 370-372, 1973.

[11] A.J. Alcock *et al.*, "Continuously tunable high pressure CO_2 laser with UV photopreionization," *Appl. Phys. Lett.*, vol. 23, pp. 562-564, 1973.

[12] N.G. Basov *et al.*,"Electric ionization lasers," *Sov. Phys. JETP.*, vol. 37, pp. 58-64, 1973.

[13] R.A. Durie and G. Herzberg, "Forbidden transitions in diatomic molecules; V," *Can. J. Phys.*, vol. 38, pp. 806-818, 1960.

[14] W.H. Christiansen and E. Greenfield, "Analysis of a collisionally induced dipole laser," *Appl. Phys. Lett.*, vol. 23, pp. 623-625, 1973.

[15] J.A. Beaulieu, "High peak power gas lasers," *Proc. IEEE*, vol. 59, pp. 667-674, 1971.

[16] A. Yariv, *Introduction to Optical Electronics*, New York: Holt, Rinehart and Winston, 1971.

[17] L.H. Aller, *The Atmospheres of the Sun and Stars*, New York: Ronald, 1963.

[18] G. Herzberg, *Spectra of diatomic molecules*, Princeton: D van Nostrand, 1950.

[19] C.M. van Atta, *Vacuum Science and Engineering*, New York: McGraw-Hill, 1965.

[20] E.E. Anderson, *Modern Physics and Quantum Mechanics*, Toronto: W.B. Saunders, 1971.

[21] H. Seguin and J. Tulip, "Photoinitiated and photosustained laser," *Appl. Phys. Lett.*, vol. 21, pp. 414-415, 1972.

[22] J. Tulip, H.J. Seguin and W. Faszer, "High repetition-rate TEA laser discharge using integrated preionization and switching," *IEEE J. Quantum Electron.*, vol. QE-12, pp. 155-159, 1976.

[23] H. Seguin, J. Tulip and D. McKen, "Ultraviolet photoionization in TEA lasers," *IEEE J. Quantum Electron.*, vol. QE-10, pp. 312-314, 1974.

[24] G.L. Clark, *Applied X-Rays*, New York: McGraw-Hill, 1955.

[25] A.H. Compton and S.K. Allison, *X-Rays in Theory and Experiment*, Philadelphia: D van Nostrand, 1954.

[26] Data provided by the New England Nuclear Corporation, Massachusetts, U.S.A.

[27] H.J. Seguin, K. Manes and J. Tulip, "Simple inexpensive laboratory-quality Rogowski TEA laser," *Rev. Sci. Inst.*, vol. 43, pp. 1134-1139, 1972.

[28] E. Nasser *Fundamentals of Gaseous Ionization and Plasma Electronics*, New York: Wiley, 1971.

[29] L.B. Loeb, "Formation of negative ions," *Encyclopedia of Physics*, Ed. S. Flugge, Berlin: Springer, 1956.

[30] G.L. Rogoff, "Gas heating effects in the constriction of a high pressure glow discharge column," *Phys. Fluids*, vol. 15, pp. 1931-1940, 1972.

[31] A.J. Palmer, "A physical model on the initiation of atmospheric-pressure glow discharges," *Appl. Phys. Lett.*, vol. 25, pp. 138-140, 1974.

[32] I. Alexeff, "Spark breakdown - an electrostatic criterion," *IEEE Trans. Plasma Sci.*, vol. PS-1, pp. 10-12, 1973.

[33] E.N. Jenkins, *An Introduction to Radioactivity*, London: Butterworths, 1964.

[34] W.P. Baxter, "Quenching of the fluorescence of Nitrogen Dioxide," *J. American Chem. Soc.*, vol. 52, pp. 3921-3927, 1930.

[35] S.E. Schwartz and H.S. Johnston, "Kinetics of Nitrogen Dioxide Fluorescence," *J. Chem. Phys.*, vol. 51, pp. 1286-1302, 1969.

[36] G. Herzberg, *Electronic Spectra of Polyatomic Molecules*, Princeton: D van Nostrand, 1967.

[37] T.C. Hall, Jr. and F.E. Blacet, "Separation of the Absorption Spectra of NO_2 and N_2O_4 in the range of 2400-5000Å," *J. Chem. Phys.*, vol. 20, pp. 1745-1749, 1952.

[38] P.G. Dickens, J.W. Linnet and O. Sovers, "Collisional energy transfer between electronic and vibrational degrees of freedom," *Disc. Farad. Soc.*, vol. 33, pp. 52-60, 1962.

[39] A.B. Callear and J.D. Lambert, *Comprehensive Chemical Kinetics*, vol. 3, Eds. C.H. Bamford and C.F.H. Tipper, New York: Elsevier, 1969.

[40] K. Sakurai and P. Broida, "Spectral Study of NO_2 fluorescence excited by 11 lines of Argon and Krypton ion lasers," *J. Chem. Phys.*, vol. 50, pp. 2404-2410, 1969.

[41] A.C.G. Mitchell and M.W. Zemansky *Resonance Radiation and Excited Atoms*, New York: MacMillan, 1934.

[42] G. Karl and J.C. Polanyi, "Infrared emission arising from electronic-vibrational energy transfer: Hg+CO," *J. Chem. Phys.*, vol. 38, pp. 271-272, 1963.

[43] G. Karl, P. Kruss and J.C. Polanyi, "Infrared emission studies of electronic-to-vibrational energy transfer: II Hg^*+CO," *J. Chem. Phys.*, vol. 46, pp. 224-243, 1967.

[44] G. Karl *et al.*, "Infrared emission studies of electronic-to-vibrational energy transfer: III Hg^*+NO," *J. Chem. Phys.*,vol. 46, pp. 244-253, 1967.

[45] A.B. Callear, "Measurement of energy transfer in molecular collisions," *Appl. Optics Suppl. on Chemical Lasers*, pp. 145-170, 1965.

[46] K.F. Herzfield and T.A. Litovitz, *Absorption and Dispersion of Ultrasonic Waves*, New York: Academic, 1959.

[47] S.R. Leone and F.J. Wodarczyk, "Laser excited electronic-to-vibrational energy transfer from $Br(4^2P_{1/2})$ to HCl and HBR," *J. Chem. Phys.*, vol. 60, pp. 314-315, 1974.

[48] A.B. Petersen, C. Wittig and S.R. Leone, "Infrared molecular lasers pumped by electronic-vibrational energy transfer from $Br(4^2P_{1/2})$: CO_2, N_2O, HCN and C_2H_2," *Appl. Phys. Lett.*, vol. 27, pp. 305-307, 1975.

[49] A.B. Petersen, C. Wittig and S.R. Leone, "Infrared molecular lasers pumped by E-V energy transfer," *IEEE Ninth Conference on Quantum Electronics*, pp. 125-126, 1976.

[50] C.A. Parr and D.G. Truhlar, "Potential energy surfaces for atom transfer reactions involving Hydrogen and halogens," *J. Phys. Chem.*, vol. 75, pp. 1844-1860, 1971.

[51] K.J. Laidler, *The Chemical Kinetics of Excited States*, Oxford: Clarendon, 1955.

[52] K.J. Laidler, "The mechanism of processes initiated by excited atoms, I. The quenching of excited Sodium," *J. Chem. Phys.*, vol. 10, pp. 34-42, 1942.

[53] K.J. Laidler, "The mechanism of processes initiated by excited atoms, II. Photosensitization by excited Mercury and Cadmium," *J. Chem. Phys.*, vol. 10, pp. 43-50, 1942.

[54] J.C. Polanyi, "Infrared Chemiluminescence," *Quant. Spectrosc. Radiat. Transfer*, vol. 3, pp. 471-496, 1963.

[55] R.B. Timmons and R.E. Weston, "Relative rates of reaction of Bromine atoms with isotopic Hydrogen molecules," *J. Chem. Phys.*, vol. 41, pp. 1654-1661, 1964.

[56] K.J. Laidler, *Theories of Chemical Reaction Rates*, New York: McGraw-Hill, 1969.

[57] P.J. Robinson and K.A. Holbrook, *Unimolecular Reactions*, New York: Wiley, 1972.

[58] S. Glasstone, K.J. Laidler and H. Eyring, *The Theory of Rate Processes*, New York: McGraw-Hill, 1941.

[59] R.A. Marcus, "Dissociation and Isomerization of vibrationally excited species, III," *J. Chem. Phys.*, vol. 43, pp. 2658-2661, 1965.

[60] J.C. Tully, "Collision complex model for spin forbidden reactions: Quenching of $O(^1D)$ by N_2," *J. Chem. Phys.*, vol. 61, pp. 61-68, 1974.

[61] D.O. Ham and J.L. Kinsey, "Long-lived collision complexes in molecular beam scattering experiments," *J. Chem. Phys.*, vol. 53, pp. 285-299, 1970.

[62] G. Herzberg, *Infrared and Raman Spectra of Polyatomic Molecules*, Princeton: D. van Nostrand, 1960.

[63] V.K. Bykhovskii and E.E. Nikitin, "Transitions associated with atomic-molecular collisions: Quenching of the resonance fluorescence of Mercury," *Opt. Spectry.*, vol. 16, pp. 111-114, 1964.

[64] C.E. Treanor, J.W. Rice and R.G. Rehm, "Vibrational relaxation of anharmonic oscillators with exchange-dominated collisions," *J. Chem. Phys.*, vol. 48, pp. 1798-1807, 1968.

[65] L.I. Schiff, *Quantum Mechanics*, New York: McGraw-Hill, 1955.

[66] G. Zener, "Non-adiabatic crossing of energy levels," *Proc. Roy. Soc., Ser. A.*, vol. 137, pp. 696-702, 1932.

[67] C. Zener, "Dissociation of excited diatomic molecules by external perturbations," *Proc. Roy. Soc., Ser. A.*, vol. 140, pp. 660-668, 1933.

[68] D.R. Bates, "Collisions involving the crossing of potential energy curves," *Proc. Roy. Soc., Ser. A.*, vol. 257, pp. 22-30, 1960.

[69] E.E. Nikitin, "Theory of non-adiabatic transitions. Recent development of the Landau-Zener (Linear) model," in *Chemische Elementarprozesse*, Ed. H. Hartman, Berlin: Springer, 1968.

[70] T.R. McCalla, *Introduction to Numerical Methods and Fortran Programming*, New York: Wiley, 1967, ch. 8, pp. 262-293.

[71] T.G. Slanger and G. Black, "Electronic-to-vibrational energy transfer efficiency in the $O(^1D) - N_2$ and $O(^1D)$ - CO systems," *J. Chem. Phys.*, vol. 60, pp. 468-477, 1974.

[72] J.L. Magee and T. Ri, "The mechanism of reactions involving excited electronic states, II. Some reactions of the alkali metals with Hydrogen," *J. Chem. Phys.*, vol. 9, pp. 638-644, 1941.

[73] H.L. Kramer and D.R. Herschbach, "Combination rules for van der Waal's force constant," *Jour. Chem. Phys.*, vol. 53, pp. 2792-2800, 1970.

[74] T. Yamanouchi and H. Horie, "Intensities of forbidden lines of atoms in p^n-configuration," *J. Phys. Soc. Japan*, vol. 7, pp. 52-57, 1952.

[75] M. Born and R. Oppenheimer, "On the quantum theory of molecules," *Ann. Phys.*, vol. 20, pp. 457-484, 1927.

[76] E.V. Condon, "The Franck-Condon Principle and related topics," *Am. J. Phys.*, pp. 365-374, 1947.

[77] R. Seiler, Does the Born-Oppenheimer Approximation work?", *Helvetica Physica Acta.*, vol. 46, pp. 230-234, 1973.

[78] M.A. Morrison, T.L. Estle and N.F. Lane, *Quantum States of Atoms, Molecules and Solids*, Englewood Cliffs, N.J.: Prentice-Hall, 1976, ch. 12, pp. 259-272.

[79] P. Pringsheim, *Fluorescence and Phosphorescence*, New York: McGraw-Hill, 1949.

[80] T.G. Slanger, C. Black and J. Fournier, "Electronic-to-vibrational energy transfer between molecules," *J. Photochem.*, vol. 4, pp. 329-339, 1975.

[81] Ref. [78], pp. 296-297.

[82] E.V. Condon and G.H. Shortley, *Theory of Atomic Spectra*, Cambridge: University Press, 1935.